8
Automated Data Processing and Quantification in Polymer Mass Spectrometry

Till Gruendling, William E. Wallace, Christopher Barner-Kowollik, Charles M. Guttman, and Anthony J. Kearsley

8.1
Introduction

The interpretation of synthetic polymer mass spectra is a process that usually requires intricate knowledge of both, the synthetic chemistry of the investigated polymers as well as the measurement process itself and the instrumentation at hand. The growing usage of mass spectrometric tools in the polymer community also leads to an increasing number of nonexpert users of the technique. Sophisticated tools for the automated processing and interpretation of mass spectra have the potential to significantly increase the acceptance of mass spectrometry (MS) as a versatile technique in polymer characterization by these users, while at the same time providing an operator-independent and reproducible outcome of the interpretation process. Especially when extracting quantitative information – for example on the compositional distribution of copolymers or the molecular mass distribution (MMD) of homopolymers – operator-independent approaches for spectral evaluation are highly desirable. Sophisticated data processing and database search tools have the potential to maximize the efficiency and accuracy of investigations by hyphenated techniques, including tandem mass spectrometry (MS/MS), ion mobility spectrometry (IMS), and online liquid chromatography mass spectrometry (LC-MS). The following sections give an overview of the techniques that are currently available to the polymer community and should guide the interested scientist in the selection of suitable tools for spectral interpretation. The reader will realize that – although tools have matured in areas such as copolymer characterization and molecular mass determination – the field of automation in polymer MS is in many areas still in its infancy.

8.2
File and Data Formats

Once the physical process of spectrum acquisition has been carried out, every data analysis effort – automated or manual – requires importing of the mass spectral data

Mass Spectrometry in Polymer Chemistry, First Edition.
Edited by Christopher Barner-Kowollik, Till Gruendling, Jana Falkenhagen, and Steffen Weidner

into a processing software suite. Here, the generated spectra are either displayed for manual interpretation by the user or further automated data retrieval, preprocessing, interpretation, and quantification steps may be performed. The current situation features a plethora of vendor-specific, proprietary data formats in MS. At times, diversity exists even between instrument generations of the same vendor, and the negative impact on scientific data exchange and efforts to automate spectral interpretation needs to be realized. Polymer mass spectra acquired by direct infusion electrospray ionization mass spectrometry (ESI-MS) or matrix-assisted laser desorption ionization mass spectrometry (MALDI-MS) without chromatographic fractionation of the sample can be stored as a two-column data matrix, and thus are easily handled in the form of simple text files for data export, which is supported by most software.

However, in the last years, a trend is also witnessed within the polymer MS community toward the realization of increasingly more sophisticated scenarios, featuring mass spectrometric analysis in combination with other means of macromolecular separation or fragmentation to maximize information content. Hyphenated techniques such as size-exclusion chromatography (SEC) or chromatography under critical conditions of adsorption (LCCC) coupled online or offline to MS as well as gas phase separation techniques such as IMS may allow more structural data to be gained from the measurements than from a simple MS experiment by itself. Tandem MS in combination with knowledge about the fragmentation pathways of certain polymer species may enhance the information gained on polymer functionality and composition. The multidimensional data obtained from these approaches requires sophisticated means for its compact storage, ideally in openly accessible data formats. In the field of proteomics, the sheer complexity of information from tandem LC/MS^2 experiments necessitates automated processing from the very beginning of the data analysis chain and sophisticated tools have therefore been developed over the last couple of years [2–4]. The requirement of a common open data format to enable the platform and instrument vendor-independent processing and exchange of data has also been realized in recent years within the proteomics community [1, 5, 6]. As a result, two open data formats have emerged, based on the extensible markup language (XML) standard: The mzXML [1] format, developed by the Seattle Proteome Center and later the mzML [5] format developed by the Human Proteome Organization's proteomics standards initiative, which aims to marry the superior elements of mzXML with a third data format, mzData [7]. Figure 8.1 shows the great benefit of this approach in that a common (open source) data analysis pipeline may be used to data analysis which uses one unified open file format as data input. Software developers will be freed from the need to obtain knowledge about the different vendor-specific formats thus enabling the development of truly universal software tools. Furthermore, common file standards will allow public storage and retrieval of data over long periods. A number of open source programs are available today to convert vendor-specific formats to mzXML or mzML files. A list of these converters can be found in Ref. [3]. Increasingly, instrument vendors are also beginning to support these open file standards.

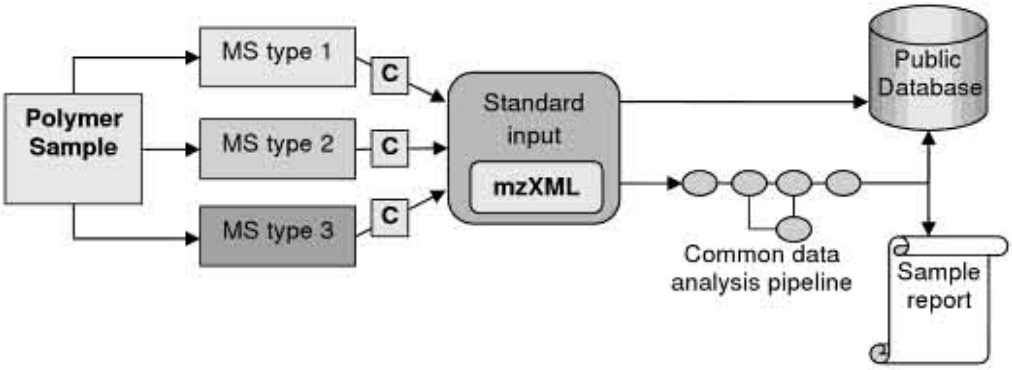

Figure 8.1 The mzXML file acts as a mediator, allowing multiple input formats to be subjected to a common data analysis pipeline. New types of instruments can be integrated into a preexisting analysis framework with only a utility (here represented by C) to convert MS native output to the mzXML format. The open structure of mzXML instance documents makes them suitable for data exchange such that, for example, they may be submitted to a data repository to support the results presented in a publication. Figure adapted from Ref. [1].

8.3
Optimization of Ionization Conditions

Finding the instrumental settings and experimental conditions at which the sensitivity and accuracy of an analytical procedure is at its optimum is one of the main goals in any analytical method development process. In MS, a great number of these chemical and instrument parameters exist that the scientist can tweak. With regards to polymer analysis by MS, depending on what the goal of the mass spectrometric experiment is, the objective to be optimized may vary. The instrumental noise and sensitivity may be important objectives in quantification studies of low abundant polymer species. Minimization of ionization mass bias and optimization of detector linearity or dynamic range are required in MMD determination by MALDI-MS [8]. Recently, the introduction of living/controlled radical polymerization protocols has lead to new kinds of functional polymers carrying end groups such as halogen atoms, dithioesters, or nitroxides which are bound to the polymer terminus by intrinsically weak carbon–chalcogen or carbon–halogen bonds. Especially with nonpolar polymers such as polystyrene [9, 10], which are difficult to ionize in general, but also with poly(methyl methacrylate) (PMMA) [11, 12], loss of these end groups is often observed in MALDI-MS. This leads to information loss and false deductions in the case of mechanistic investigations or when MS is used to verify end-group fidelity. ESI has the advantage that it often provides a much softer ionization of the polymer molecule, with full retention of functionality [12, 13], but in a few cases, end-group losses for polymers synthesized by living/controlled radical polymerization have been observed even with ESI-MS [10]. The retention of functionality is therefore a third important objective in polymer MS requiring optimization, especially when mechanistic and structural studies are to be performed.

The physical processes affecting the performance of the ionization source, mass separating process, and ion detection are often only insufficiently understood and conditions depend critically on the type of mass spectrometer employed. With only little or no *a priori* knowledge of the optimal conditions, the number of parameter settings to be sampled is very large. Often, source optimization in both MALDI-TOF and ESI-MS is performed in a one-factor-at-a-time fashion [14]. This approach, although straightforward to perform, may not yield the best experimental conditions, as interactions between parameters cannot be identified [15, 16]. Design of experiment (DoE) is a useful tool that can be employed to significantly reduce the number of the experiments required in optimizing ionization conditions, while retaining maximum certainty in the effects of the experimental parameters and their interactions on arbitrary objectives to be optimized. Response surface designs allow the statistical and graphical evaluation of the experimental data by regression analysis with suitable model functions [15, 17, 18]. A number of different applications of DoE to LC-MS optimization exist in literature, many covering the optimization of the liquid chromatographic separation [19, 20], but some also covering the optimization of MS source conditions [18, 20, 21]. More recently, Kell and coworkers successfully employed a genetic search method [22] to achieve an operator intervention-free, fully automated numerical optimization of up to 14 instrument settings in polypeptide ESI-MS [23] and gas chromatography-MS [24]. These authors noted that the method could yield optimum conditions by sampling less than 500 of the possible 10^{14} combinations and that relationships between source parameters were identified that accounted for much of the success of the optimization. The hypothesis-generating potential of genetic search processes in which little *a priori* knowledge of the system is available was thus demonstrated.

A selection of articles exist that are directly related to polymer MS. Wetzel *et al.*, for example, employed an orthogonal experimental design to identify parameters that significantly affected signal-to-noise ratio in polystyrene analysis by MALDI-TOF-MS. From a set of five parameters including detector voltage, laser energy, delay time, extraction voltage, and lens voltage, detector voltage and delay time were shown to be the most influential [25]. Later, Wallace *et al.* employed numerical optimization routines to find conditions of minimal instrumental mass bias, which is one goal when employing MALDI-MS to generate absolute MMD standards. Stochastic numerical optimization [26, 27] was employed to this task, and the effects of instrumental noise on the optimization procedure were dealt with by the use of implicit filtering [28]. Optimal values of five instrument parameters were obtained in as few as five iterations and the confidence intervals of the parameters were gained which may serve for a sensitivity analysis of the effects of each parameter.

DoE can be especially useful when optimizing online LC-MS of synthetic polymers. Here, the operator is faced with the challenge of having to find optimum ionization conditions in a system where the concentration of analytes eluting from a chromatographic column is changing rapidly as a function of time. In such cases, parameters may need to be varied between chromatographic runs with the goal to obtain maximum information from a minimum amount of chromatographic runs to save valuable instrument time. Gruendling *et al.* presented a method based on a

D-optimal design, which allows for a modification of the number of experiments included in the design plan [29]. The influence of four ionization source parameters, including cone voltage, spray gas flow rate, and capillary temperature on ionization efficiency and their optimum settings were identified.

In MALDI-MS, the selection of proper conditions for sample preparation including the correct chemical matrix, solvents, and ionization salt in suitable concentrations is a crucial part of the signal optimization process. A number of studies exist in this direction, with one very interesting approach by Schubert and coworkers [30]. These authors used quantitative structure–performance relationships for the rational selection of potentially new well-performing matrices for MALDI of synthetic polymers. Recently, Brandt *et al.* [31–33] employed partial least square regression together with a training set of eight matrices, five cationization reagents and six solvents to predict the performance of untested combinations of matrix, cationization reagent and solvent. Molecular descriptors were used for the matrix and cationization reagent, while Hansen solubility parameters were found to be the most informative for the solvent. The authors concluded that, despite of inconsistencies due to the formation of precipitates with some salts, the established structure–performance relationships may serve as a starting point to predict the performance of matrices in the case of unknown polymers.

8.4
Automated Spectral Analysis and Data Reduction in MS[1)]

Numerical spectrum analysis is an often neglected subject in the overall study of MS. It is typically treated as an afterthought to the widely studied subjects of sample preparation, ionization mechanisms, and mass-to-charge separation methods. Yet it is the determination of accurate and precise peak positions that is at the core of chemical identification in MS. Furthermore, it is the determination of peak intensity that underpins any quantitative measurements. This section presents, in brief, two new methods that have been developed at the National Institute of Standards and Technology. These methods make no assumptions about peak shape.

Mass spectral "peaks" are defined as statistically significant excursions in the spectrum intensity from its baseline that are the result of ions of a given mass-to-charge ratio (m/z) being detected by the instrument. Spurious peaks may arise from purely random events of either electronic or chemical origin. Electronic noise arises from the detector, preamplifier, amplifier, or spectrum digitizer. Chemical noise arises from stray ions that have been improperly separated in time, mass, or kinetic energy. Typically spectrum averaging will smooth out such peaks if the noise is truly random and uncorrelated. Spurious peaks may also arise from systematic instrument artifacts, for example, periodic effects such as digitizer jitter (yielding electronic noise) or voltage fluctuations (leading to chemical noise). From a purely

1) Official contribution of the National Institute of Standards and Technology; not subject to copyright in the United States of America.

statistical or numerical point of view, these may be impossible to distinguish from genuine peaks. The analyst needs answers to the following questions:

1) When is a given excursion correctly classified as a genuine peak? (statistical significance)
2) At what m/z is the peak most likely located? (peak location)
3) Does it overlap with other nearby peaks? (peak resolution)
4) Where does a peak begin and end? (integration end points)
5) What is the area of the spectrum underneath the peak? (peak integration).

An answer to the first question is used to separate true peaks from spurious peaks. An answer to the second question is required for species identification and is used predominantly in qualitative analysis. The third question must be answered to determine if two or more peaks overlap as a result of insufficient mass-to-charge resolution. Overlapping peaks may lead to incorrect peak position and intensity determination. Knowledge of the location of the peak beginning and end, the fourth question, is required to determine peak area. Peak area, in turn, is typically required for quantitative analytical results. Succinct answers to these questions will result in a reliable translation between the spectrum and the metrics the analyst wishes to determine. Failure to properly answer these questions renders moot efforts at sample preparation and data collection.

8.4.1
Long-Standing Approaches

Standard approaches to the reduction of mass spectral data have focused on calculating either derivatives or intensity thresholds of the data. A few of the many reviews in the literature can be found in Refs. [34–37]. Typically, excursions from the baseline are found at increases in the first derivative. As the algorithm proceeds sequentially through the data (typically but not necessarily from low m/z to high m/z), an initial excursion of the derivative, or an increase in intensity above a preset threshold, indicates a peak beginning. A peak maximum is found when the derivative after an initial increase flattens out to zero. As the algorithm proceeds sequentially, the derivative will change sign and then flatten out to zero again, or the intensity will drop below the preset threshold value, as the baseline is restored.

Many variations of this basic method exist. For example, second derivatives may be used to find peak maxima. In some cases, third derivatives may also be employed. There are two significant problems that one encounters when using these derivative-based approaches. First, the function whose derivative must be approximated is only available at discrete prescribed points, that is, one has access only to (x, y) pairs of data, not to a continuous function. Second, random noise results in inaccurate derivative estimates. It is well known that the availability and accuracy of derivative approximations decreases as noise in a function increases. The result is that noisy data, when analyzed with algorithms that employ derivative approximations, may fail to find genuine peaks and may identify as peaks features that are purely artifacts. Furthermore, the higher the derivative, the greater its sensitivity to random noise [38].

In this case, smoothing or filtering of the data is one way to ensure existence and computability of needed derivative estimates. Running or windowed averages, Savitsky-Golay smoothing [39–41], Fourier filtering [42], and wavelet decomposition [43] are the most common of the many methods possible and have been extensively discussed in the literature. However, the success of these methods relies on a circular logic in which the type and degree of smoothing determine the effectiveness of the peak finding algorithm, and the effectiveness of the peak finding algorithm determines the amount of smoothing required. The problem is compounded when the noise is variable across the m/z range, or when the noise is not constant between spectra but the analyst wishes to apply to same data analysis methods to all spectra of a series. Different kinds of, or degrees of, smoothing may be required in different parts of the spectrum. Likewise, derivative computation (or other gradient estimates) may be more feasible in one part of the spectrum than another.

8.4.2
Some New Concepts

Many of the new concepts in peak identification and integration attempt to move beyond the purely local approaches of derivatives or thresholds. Furthermore, they attempt to do this without going toward global spectrum smoothing. Here "local" refers to operations on any given mass versus intensity (x, y) data point and its nearest neighbors. "Global" refers to operating on the spectrum as a whole without consideration of any specific local features, such as Fourier filtering. New methods endeavor to treat the spectrum as a series of regions that are larger than a few data points but smaller than the spectrum as a whole. They attempt to isolate peaks into "neighborhoods" or small sets of mass versus intensity data points. By analogy, the spectrum is the city, the peaks are its neighborhoods, and the data points are individual addresses.

8.4.3
Mass Autocorrelation

Signal autocorrelation has an extensive history in the communications field [44]. The mass autocorrelation function, $G(L)$ is defined as

$$G(L) = \frac{\sum_i S(m_i) \cdot S(m_{i+L})}{\sum_i S(m_i)^2} \tag{8.1}$$

where $S(m_i)$ is the signal at mass m_i taken on equal intervals of mass, Δm, and L is the lag which is also measured in units of mass. Equal intervals of mass are used because most correlation algorithms require the signal to be evenly spaced points on the scale of interest. As an aside, remember that in TOF mass separation, the signal, $S(t_i)$, is collected on equal intervals of time. The transformation from this time-base signal

$S(t_i)$ to a mass-base signal $S(m_i)$ involves both an interpolation and a change of the signal itself by a Jacobian transform. The mathematical methods to effect this transformation are discussed in Ref. [45]. Numerical interpolation must be used to convert the spectrum in mass from unequally spaced points to equally spaced points for the application of autocorrelation methods. By choosing reduced (contiguous) sets of the data, information about periodic peaks may be obtained in as local or as global a context as desired. The periodicity of the peaks may arise from the periodic nature of the polymer's structure such as repeat units periodicity or isotopic periodicity.

In addition to verifying the mass of any repeat units found in the sample, there are several important applications of mass autocorrelation to the analysis of polymer mass spectra. By autocorrelating in different regions of the data, and by overlaying these results, subtle changes in polymer architecture can be discovered. This was demonstrated for polysilsesquioxanes where the degree of intermolecular condensation could be quickly and accurately tracked without having to resort to identifying every peak in the spectrum [46, 47]. A second application involves pulling a weak signal out of noisy data [45]. Exploiting the fact that for a polymer there should be a repeating peak sequence at the repeat unit mass, autocorrelation can reveal if the expected polymer ions have been detected in an otherwise noisy spectrum. Figure 8.2 shows a very noisy polystyrene MALDI-TOF spectrum. Identifying the mass difference between pairs of peaks is difficult. Autocorrelation compares intensities at all

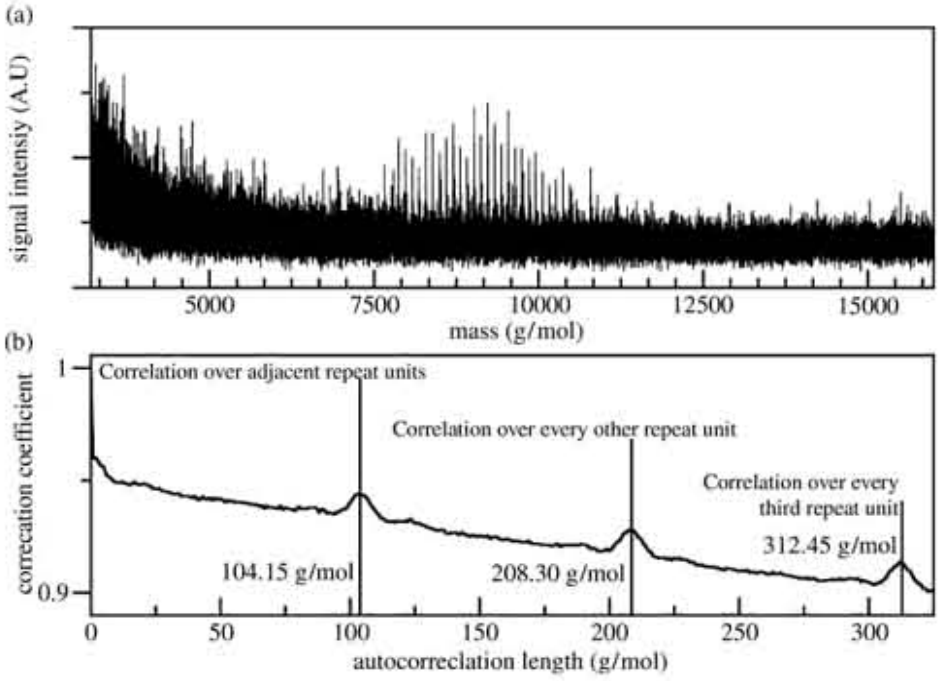

Figure 8.2 Autocorrelation applied to noisy polymer mass spectrometry data. (a) Mass spectrum. (b) Autocorrelation function. Notice the clearly repeating structure at 104.15 g mol^{-1} which is the repeat unit mass of polystyrene.

mass differences across the spectrum. In cases with matching peak distances the autocorrelation coefficient increases. This can be seen in the figure where correlations of peaks one, two, or three repeat unit masses apart are clearly seen and the repeat unit of polystyrene is clearly identified. Careful inspection of Figure 8.2 also shows small peaks on either side of the main autocorrelation series. These are due to either a separate set of end groups or adduct formation. In either case, finding this effect by simple inspection of the original spectrum would be exceedingly difficult. The third application is to mass calibration. If the repeat unit mass of the sample is known, autocorrelation can be used to adjust the slope (but not the offset) of the calibration curve. This serves to improve mass accuracy because if the slope can be corrected, then the peak positions are more accurate. This is important when calculating end group or adduct masses.

A software tool (PolyCalc) which has recently been introduced by Luftmann and Kehr allows the molecular masses of repeating units and end groups, as well as an approximation of the MMD to be obtained from the multiply-charged spectra recorded in direct infusion ESI-MS [48]. The software operates by minimizing the difference between a simulated mass spectrum and the measured ESI spectrum and thus yields the monomer and end-group mass and estimates of the MMD of the polymer, which is assumed to be Gaussian in shape. The software seems to be a useful tool effectively extending the mass range of ESI-MS to around 10–20 kg mol^{-1} if multiple charging is achieved. Programmatic extensions are needed to allow the analysis of mixtures of multiple end-group-carrying polymers.

8.4.4
Time-Series Segmentation

Another alternative to calculating local derivatives is to consider the spectrum as a whole and to reduce it to a set of concatenated line segments based on its features. As shown in Figure 8.3, by connecting the first (x, y) pair to the last (x, y) pair in the spectrum, a crude baseline for the entire spectrum is created. From this line, the (x, y) pair that is the greatest normal distance from the line is determined. This yields two line segments spanning the spectrum. This procedure is continued until the spectrum is replicated by a series of line segments with each peak determined (at the minimum) by two line segments and the intervening baseline determined (also at a minimum) by a single line segment. After the spectrum has been segmented, least squares or orthogonal distance regression [49] may be used to adjust the line segments to best fit the data; however, caution must be exercised because if the random noise level varies across the spectrum the quality of the fit will also vary across the spectrum. For this reason, the NIST method [50] uses a background spectrum taken at the same instrumental conditions as the spectrum to be analyzed with a sample that is free of analyte (e.g., in the case of MALDI, contains the matrix and the cationizing salt). A background spectrum requires additional experimental effort but yields significant dividends when analyzing the data to determine quantitative measures.

A nonlinear programming algorithm using an L2 (least squares) approximation to an L1 (least absolute-value) fit was employed [51–55]. L1 fits are superior to L2 fits due

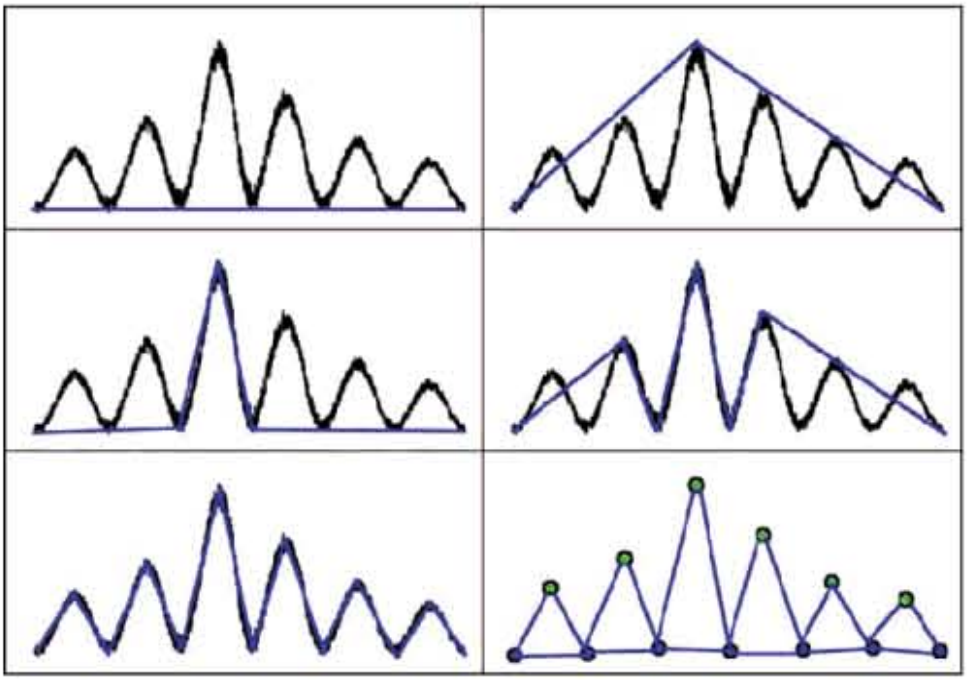

Figure 8.3 Schematic representation of time-series segmentation on a model problem. In the final panel, the green circles represent peak positions, and the blue circles represent peak beginnings/endings. The calculated relative area for each peak is the area of the triangle but many other area-summing routines are possible.

to their increased tolerance for outliers, that is, outlying points do not exert as much control over the final fit. Given a dataset of N points, a collection of strategic points is found and the unique optimal piecewise linear function passes through the x coordinate of each strategic point. This defines a set of function maxima and minima corresponding to the peak maxima and the peak limits, respectively. The original data is then integrated by finding the area of the polygon determined by the strategic points.

Our segmentation method is a two-step algorithm. The first portion requires the selection of strategic points and is derived from the earlier work of Douglas and Peucker [56]. Strategic points are selected based on an iterative procedure that identifies points whose orthogonal distance from the end-point connecting line segment is the greatest. Once a point with greatest orthogonal distance from the mean has been identified, it joins the collection of strategic points and, in turn, becomes an end point for two new line segments from which a point with greatest orthogonal distance is found. This numerical scheme is performed until the greatest orthogonal distance to any end-point connecting line segment drops beneath a prescribed threshold value. This threshold value is the only algorithmic parameter and is based on a statistical analysis of the data and its corresponding analyte-free spectrum. Clearly the selection of these points does not require equally spaced data; therefore, the method is equally well suited for TOF data expressed in either time or mass space. Generally, it is chosen to work in time space with the data in its most

basic state and to eliminate for doing a point-by-point correction of intensity using partial integrals [45]. The second phase of the algorithm, developed specifically for this work, requires the solution of an optimization problem, specifically, locating strategic point heights (i.e., adjusting strategic point y-axis values at their associated strategic x-axis values) that minimize the sum of orthogonal distance from raw data. This problem is a nonlinear (and nonquadratic) optimization problem that can be accomplished quickly using a recently developed nonlinear programming algorithm [57].

The algorithm works as shown in Figure 8.3 [50, 54]. Clearly this method requires no knowledge peak shape and no preprocessing of the data (e.g., smoothing), nor does it require equal spacing of data points. Note that the strategic points defining the beginning and end of adjacent peaks are located in the same spot resulting from the choice of $\cos^2(x)$ as the underlying function for this demonstration of the procedure.

Once the data set is fully segmented, strategic points are discarded in accordance with the statistical analysis of the original data set and its corresponding analyte-free data set. This "deflation" of strategic points using statistics-derived thresholds is performed by first analyzing the analyte-free spectrum for peaks and peak areas. Once a collection of peaks and peak areas has been accumulated, the spectrum with sample is then analyzed. Each peak identified from the spectrum with analyte is compared to peaks found in close relative proximity from the analyte-free spectrum algorithm output (i.e., peaks that appear with similar time or mass coordinates). If any peak in the spectrum with analyte has a smaller peak height or smaller peak area than most (about 95%) of the background-spectrum peaks in close proximity, then that peak is ignored. Likewise, any peak that falls outside the statistically significant measure for area and height is also discarded. Thus, no peak is identified from the sample spectrum that could have been identified by height or by area from the background spectrum. This discarding of strategic points also serves to prevent the inadvertent subdivision of larger peaks into a set of smaller peaks. This can sometimes occur if the noise in the analyte spectrum is much greater than the noise in the corresponding background spectrum.

Once the final set of strategic points has been found, the area of the polygon defined by these points is calculated. (The polygon is often, but not always, a triangle. The algorithm will work on polygons of any number of vertices connected by line segments.) The line connecting the first and last strategic points for a given peak determines a "local baseline." The mathematical basis for the polygonal area calculation algorithm is Green's theorem in the plane and can be interpreted as repeated application of the trapezoidal rule for integration [58]. The method returns the exact area of the polygon.

Figure 8.4 shows an example of a MALDI-TOF mass spectrum of polystyrene having three different end groups. Without user intervention, but with the requirement of a background spectrum for statistical deflation of the number of peaks, the algorithm is able to identify and integrate peaks without smoothing or making any assumptions on peak shape. In this case, the areas calculated from the triangular shapes defined by the three strategic points for each peak were calculated. However,

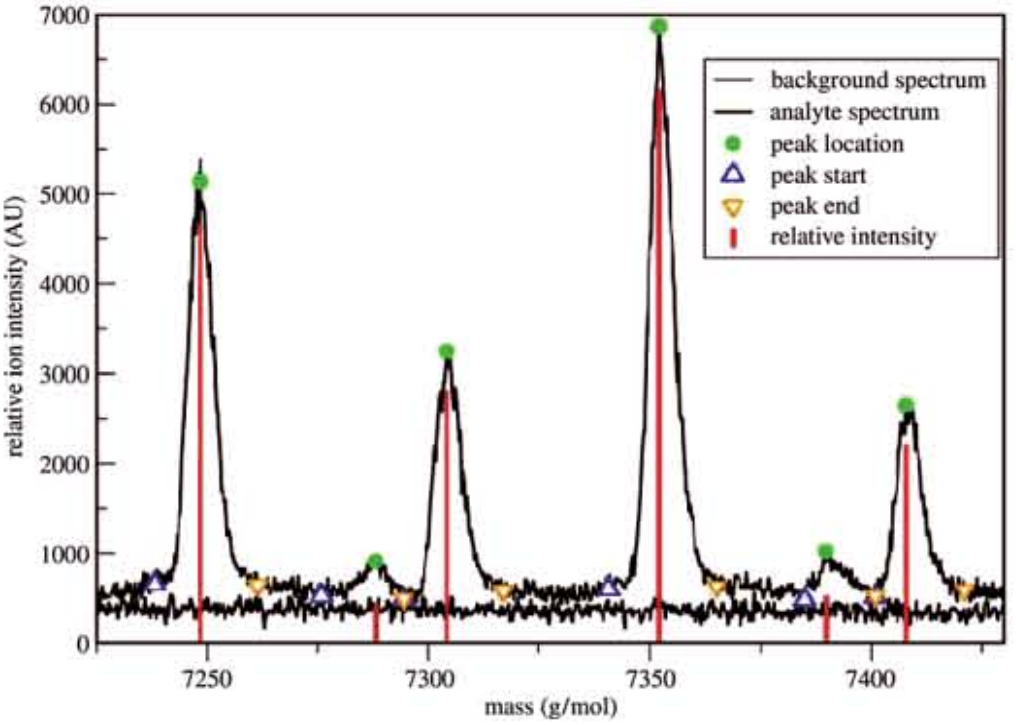

Figure 8.4 Time-series segmentation applied to real polymer MALDI-TOF mass spectral data. Note that the background spectrum has been shifted down slightly for clarity.

any method to determine the area is suitable, for example, simply summing the signal channels between the beginning and ending strategic points defining each peak.

8.5 Copolymer Analysis

The practical details and applications of soft ionization MS to analyze copolymer structure have been discussed in a preceding chapter and shall not be reiterated here. MS can serve two purposes in copolymer characterization; in addition to a determination of the end-group structure, it is possible to glean the copolymer composition from a mass spectrum (a sequence determination may be attempted after partial degradation or via MS/MS). The last two decades have seen the development of a number of mathematical approaches and software tools aimed at a spectral interpretation of copolymer mass spectra (consider also Chapter 9.9 for an alternative viewpoint on the topic). Mass spectra of copolymers are significantly more complex than homopolymer spectra. This is owing to the fact that where the MMD of homopolymers is a one-dimensional function of one repeat unit length, copolymers feature a two-dimensional topology distribution of the chain lengths of two (or multiple) monomer-building blocks.

The monoisotopic m/z of a copolymer ion in charge state z featuring m units of monomer M1 with mass m_{M1} and n repeat units of monomer M2 with mass m_{M2} and with a combined end-group mass m_E is given by the following equation:

$$m/z = \frac{m \cdot m_{M1} + n \cdot m_{M2} + m_E}{z} + m_{M+} \tag{8.2}$$

where mM+ is the mass of the adduct metal cation.

Spectral interpretation can be attempted in a generally very straightforward manner: If a hypothesis about the constituent monomers and the end group of the polymer can be made, the resultant copolymer spectrum can be modeled based solely on Eq. (8.2). A problem, however, arises, as the two-dimensional topology distribution is projected onto a one-dimensional mass spectrum, which in most cases leads to loss of information. This is due to the fact that different combinations of m and n can lead to the same or very similar m/z. Consider the example of $m_{M1} = 100$ Da and $m_{M2} = 40$ Da: A polymer with constitution $m = 4$ and $n = 10$ will feature the same mass-to-charge as one with $m = 6$ and $n = 5$. Further complication arises, as each copolymer features a distribution of masses due to the isotope distribution of ^{13}C atoms making up the backbone of the polymer and the limited instrumental resolution. Nevertheless, in the majority of cases, quantitative data may be extracted on the copolymer composition and topology distribution, given that the effects of mass bias on the ionization of copolymers with differing composition can be neglected.

Mathematical tools developed from the early 1990s for the quantitative interpretation of copolymer spectra have been accounted for in an extensive review by Montaudo [59]. This early work focused mainly on the application of chain-statistical models of the copolymerization process. The use of chain statistics to simulate a theoretical copolymer topology distribution can aid spectral interpretation by comparison of a model spectrum with the spectrum measured in reality. It was shown that using MALDI-MS with appropriate chain models, the average monomer composition, c of copolymers could be determined [60–63]. An evaluation by a direct method in which no assumptions about the polymerization process are required is also possible using the following equation [60, 64–66]:

$$c_{M1} = \frac{\sum_m \sum_n m \cdot (I_{m,n})}{\sum_m \sum_n m \cdot n \cdot (I_{m,n})} \tag{8.3}$$

where $I_{m,n}$ is the mass spectral intensity at the mass corresponding to a co-oligomer with m and n repeat units of the respective comonomers. The authors, however, cautioned that inaccuracies result when the tallest peaks in the spectrum are due to chains of less than 10 repeat units in length. Erroneous results will also be obtained in the case of strongly overlapped mass spectral peaks with ambiguous assignments in which case pruning methods have been employed [67]. The naturally occurring isotope distribution and mass-dependence of the instrumental resolution need to be corrected for if peak apices are compared instead of area ratios.

Wilczek-Vera *et al.* were among the first to demonstrate that results from MALDI-MS can be used to determine the full two-dimensional distribution of copolymer composition and chain lengths [67–69]. These authors also employed random coupling statistics in the case of block-copolymer formation to aid quantitative spectral interpretation. Their work was later followed up by Suddaby *et al.* [70] and recently by Willemse *et al.* [63, 71] and Huijser *et al.* [72, 73] who used the results for the determination of reactivity ratios in free radical copolymerizations [63, 70, 71] as well as for the mechanistic investigation of polycondensation reactions [72, 73]. These authors also derived so-called fingerprint plots (see Figure 8.5) from the mass spectra. These plots depict the two-dimensional contour plots of the probability distribution of both comonomer chain lengths as determined from the mass spectra. They provide a facile means to interpret the polymer mass spectrum and the form of the distribution observed also allows deductions to be made about the type of the analyzed copolymer (block vs. random) [74]. Weidner *et al.* recently employed the

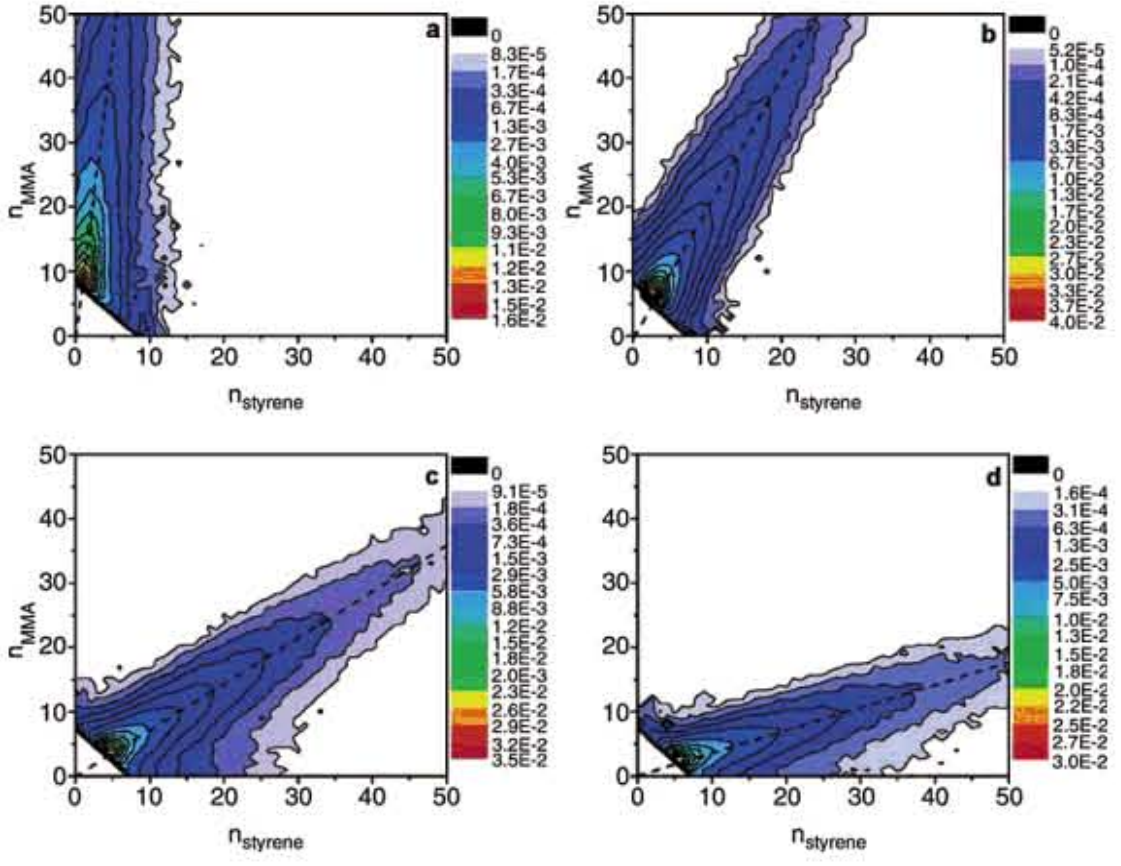

Figure 8.5 Copolymer fingerprint plots obtained from the pulsed laser-initiated radical copolymerization of MMA and styrene at a molar feed ratio (x_{St}) of: $x_{St} = 0.053$ (a), $x_{St} = 0.249$ (b), $x_{St} = 0.600$ (c), and $x_{St} = 0.792$ (d). The dashed lines in the copolymer fingerprint plots are indicative of the average chemical composition of the copolymer. The figure is taken from Ref. [71] with permission from the American Chemical Society.

method to cases in which an online coupling of MALDI and ESI MS to chromatographic separations was required and reported the introduction of a software tool developed in-house (MassChrom2D) [75, 76].

By employing a procedure named strip-based regression, Vivó-Truyols *et al.* [77] provided for the first time an elegant and statistically sound algorithm for the determination of the topology distribution of copolymers from their highly overlapped spectra in MALDI-MS. The characteristic of the algorithm to use strips whose width is a fraction of the full-acquired mass range for processing allows the data extraction problem to be treated by linear regression methods, whereas changes in the instrumental resolution of the instrument with mass-to-charge and an incorrect calibration do not deteriorate the results. As a further benefit, the application of the regression approach allows the error associated with the relative abundance of each comonomer combination to be determined.

8.6 Data Interpretation in MS/MS

Advanced fragmenting techniques in MS have been around for some while and have been extensively used in the determination of polypeptide sequence by bottom-up proteomics [78, 79]. The unambiguous interpretation of the very information-rich spectra obtained from MS/MS is greatly facilitated by the availability of highly advanced data processing software and database search tools, which are an indispensable part of contemporary proteomics [3, 4]. In recent years, MS/MS has also become a topic of largely increasing popularity in the field of synthetic polymer characterization. The fragmentation pattern of macromolecules can provide detailed information on the structure of the constituent monomer-building blocks as well as on the attached end groups. A number of studies have established the main degradation pathways of common polymers such as PMMA, poly(butyl methacrylate), poly(ethylene glycol), poly(propylene glycol), poly(styrene), poly(2-ethyl-2-oxazoline)s, and poly(α-methyl styrene) [80–94]. Software for the automated interpretation of synthetic polymer tandem mass spectra may prove to be a valuable tool for the determination of the backbone structure and end groups of otherwise uncharacterized polymers as well as for the analysis of the chain structure of copolymers. The advances in software development and the large availability of open source software solutions in biomolecular MS may greatly benefit development of suitable tools for synthetic polymer MS/MS. So far, there is only one tool available developed by Thalassinos *et al.* [95] that, however, greatly aids interpretation of tandem mass spectra and which is provided free of charge by the author. A screenshot of the software is given in Figure 8.6. Taking user-provided input on the repeating monomer units and the α- and ω-end-groups as well as the type of the attached cation, the software automatically assigns the recorded peaks to fragment ion species, followed by a color coding of the peaks making further spectral interpretation highly intuitive. Tentative assignments of the end groups can be quickly validated, which

Figure 8.6 Screenshot of the polymerator software showing an annotated expansion (m/z range 490–1350 Th) of the ESI-MS/MS spectrum of the lithiated octadecamer of PMMA. Details of annotated fragment ions are displayed by the software in the table below the spectrum. Predicted fragment ions are also detailed above (left) of the spectrum.

otherwise poses a time-consuming process. The authors have also reported on the application of Polymerator to analyze PPG [96] and poly(hydroxyethyl methacrylate) [97].

8.7 Quantitative MS and the Determination of MMDs by MS

MS with soft ionization has evolved into a powerful analytical tool in macromolecular science within the last two decades. MALDI-MS [98] and ESI-MS [99] are especially versatile tools for the analysis of synthetic polymers. A large field of application of MS in polymer science aims at gaining qualitative information on the chemical identity of the repeat units or end groups of a synthetic macromolecule based on the precise measurement of the molecular weight of individual oligomer molecules. Although MALDI-MS and ESI-MS yield exact molecular weights of individual molecules, accurate MMD of synthetic polymers requires sophisticated spectral processing approaches. This is because, intrinsically, synthetic polymers do not exhibit one

uniform chain length but rather a distribution of molecular weights. Although in MS, the molecular weight axis is certain, due to instrumental bias and a dependence of ionization efficiency on molecular weight and charge state, abundances of oligomer ions are not an accurate description of oligomer concentration in the analyzed sample. Classical methods used for the determination of MMDs by SEC yield accurate information about the concentration of the polymer. The molecular weight axis though is uncertain in SEC and existing calibration procedures may introduce errors of up to 30% in the obtained molecular weights [100].

In the following text, two approaches, developed independently at the National Institute of Standards and Technology [101] and at Karlsruhe Institute of Technology [102, 103], respectively, are described and evaluated. The first approach (see Section 8.7.1) has been employed in the context of creating an absolute molecular mass standard (Standard Reference Material™ (SRM) 2881) from MALDI measurements alone, using an internal calibration of the mass spectral intensity axis [101]. The second approach (see Section 8.7.2) relies on the use of SEC coupled online to a quantitative concentration detector (refractive index (RI) detector), whereas molecular mass calibration and band-broadening correction are achieved using peak data obtained from online ESI-MS [102, 103].

8.7.1
Quantitative MMD Measurement by MALDI-MS[2)]

The accuracy of a polymer's MMD determined from a well-resolved mass spectrum depends on accounting correctly for the mass bias in the measurement. Here "well-resolved" means having the ability to separate to baseline the individual peaks of two oligomers whose mass differs by one unit of their (typically) periodic mass spacing.

This ability is required for the quantitation methods described in this section. The methods found here have been developed at the National Institute of Standards and Technology and are described in more detail in Refs. [101, 104–106]. Mass bias is the systematic over- or undercounting of specific parts of the MMD by the mass spectrometer. Here "specific parts" can refer to the high-mass or low-mass parts of the spectrum, or to specific types of oligomers as defined by, for example, end group or molecular architecture. Mass bias can occur in any of the three basic functions of the mass spectrometer (sample ionization, separation by m/z, and detection) as well as in the sample preparation or the data analysis. By systematic it is meant that the bias is an inherent aspect of the measurement and how it is conducted and not simply due to imperfect counting statistics. In the latter case, taking more data will resolve the problem; in the former case, taking more data is not a viable solution. For systematic bias, the magnitude of the bias must be found and a correction is applied, otherwise the measured MMD is of little use.

Fundamental metrological principles identify two types of measurement uncertainty, type A and type B. Type A refers to uncertainty that can be evaluated by the

2) Official contribution of the National Institute of Standards and Technology; not subject to copyright in the United States of America.

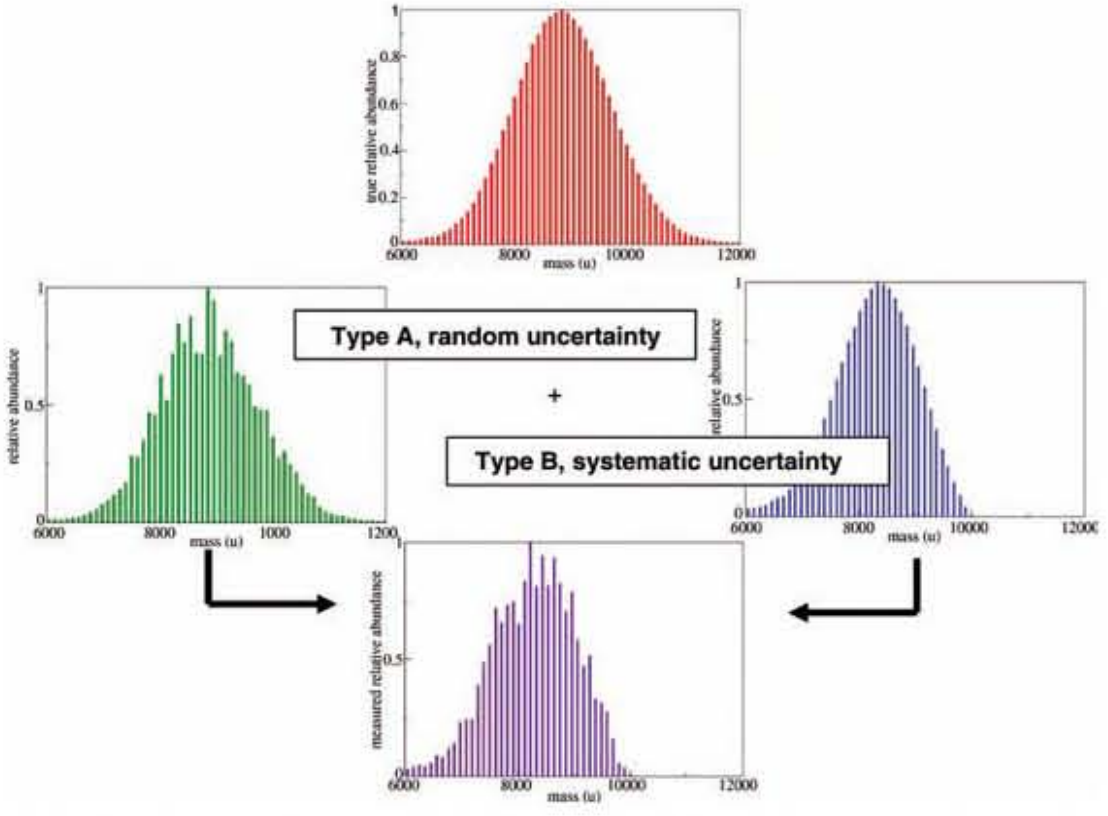

Figure 8.7 Schematic illustration of type A ("random") and type B ("systematic") uncertainties in MMD measurement.

statistical analysis of a series of observations, whereas type B refers to uncertainty that cannot be evaluated by statistical methods alone. Generally, type A is spoken of as *statistical* or *random* uncertainty and type B as *systematic* uncertainty. Their differences applied to the MS are shown in Figure 8.7. This section is concerned with the determination of type B. Type A uncertainty that can be determined (and reduced) by repeat measurements is not explicitly discussed here. It is noted that measurement repeatability is critical. If the operator cannot repeat the measurement from run-to-run and from day-to-day, the chances of measuring the correct MMD decrease dramatically. The measurement method must be repeatable and reliable before it can be considered for quantitative, much less for standards, work.

An MMD is a two-dimensional quantity of which the mass spectrum is its (imperfect) representation. Thus, both the mass axis and the signal axis (i.e., the intensity of the ion signal at any given mass) have to be calibrated separately, and their associated type B uncertainties are considered separately.

Mass axis quantification is the most easily performed of the two and is not a significant source of uncertainty in determining the MMD from the mass spectrum. Calibration of most mass spectrometers is usually done with biopolymers of known molecular masses. These biopolymers are selected because they typically provide a single major peak whose mass is known accurately; thus, mass axis quantification is

quite straightforward. Calibration must be done using at least two or three of these biopolymers that span the mass range of interest. More calibration points would increase calibration accuracy. Calibration of the mass axis can also be done by combining a single biopolymer with a molecular material calibrant. If this material is close to, or identical to, the material under study then, in general, inaccuracies in mass axis calibration will be minimized. The oligomeric masses, m_i, with n repeat units of mass r and masses of the end group, m_{end}, of the polymer calibrant are given by

$$m_i = nr + m_{end} + m_{adduct} \tag{8.4}$$

where m_{adduct} refers to the mass of any charged or neutral atoms or molecules noncovalently bound to the analyte. This may be, for example, any salts added to the sample preparation to encourage charging of the analyte. Thus, calibration of the mass axis using a homopolymer calibrant (for example) reduces to determining n for one of the peaks. A mass accuracy of better than a few mass units is not necessary since polymer MMDs are not critically dependent on such small mass differences.

Calibration of the signal axis is much more difficult. There are many systematic uncertainties that can arise in the signal axis quantitation. It would be an insurmountable task to try to quantify each of these uncertainties individually. Instead, the systematic bias in the signal axis is best determined heuristically by gravimetric techniques. By mixing together in carefully prepared gravimetric ratios samples having different MMDs, a mixture's MMD can be controlled. By comparing the gravimetric ratios to the signal intensity in the mass spectrum, a calibration curve for the signal axis can be obtained.

Various averages, known as molecular moments, where the entire shape of the distribution is reduced to a single number, serve as useful numerical simplifications of the MMD. Measuring and computing these summary statistics has historically comprised the core of the analysis of molecular materials. The two most common measures of the MMD are the number-average molecular mass, M_n, and the mass-average molecular mass, M_w.

$$M_n = \frac{\sum_i m_i n_i}{\sum_i n_i} \tag{8.5}$$

$$M_w = \frac{\sum_i m_i^2 n_i}{\sum_i m_i n_i} \tag{8.6}$$

$$\mathrm{PD} = \frac{M_w}{M_n} \tag{8.7}$$

where m_i is the mass of a discrete oligomer i, n_i is the number of molecules at the given mass m_i, and PD defines the polydispersity (PD) index.

To estimate the level of uncertainty in an instrumental method, a mathematical construct is needed to determine how type B uncertainties affect the final measurand. Assume that there is a point in the experimental parameter space (sample preparation, instrument operation, and data analysis) where the signal intensity, S_i, for an oligomer of mass m_i is linearly proportional to n_i, the number of polymer molecules at that oligomer mass. Mathematically, this is given by

$$S_i = kn_i \tag{8.8}$$

where for a narrow enough range of m_i, it is assumed that k is a constant independent of m_i and the range of linearity, $n_i < n_0$, is about the same for all molecules in the (polydisperse) sample.

If the measurement is performed in the linear region for all the oligomers of the sample, the overall signal from the quantity of analyte introduced into the mass spectrometer is given by

$$\sum_i S_i m_i = k \sum_i n_i m_i \tag{8.9}$$

with $n_i m_i$ summed over all i. From this, it can be derived that

$$\frac{\sum_i S_i m_i}{\sum_i S_i} = \frac{k \sum_i n_i m_i}{k \sum_i n_i} \tag{8.10}$$

The right-hand side of the equation is by definition the exact M_n of the polymer independent of k since k in numerator and denominator cancels out. The same holds for equations for M_w and all higher moments. This is generally true when the measurements are made in the linear range of analyte versus signal strength. However, it is well known that the mass spectra of wide PD analytes give poor representations of the MMD due to large systematic uncertainties in the signal axis. That is, if the values of the m_i span too great a mass range, then the values for k and/or the n_0 saturation limits must change dramatically, otherwise MS would be able to obtain the MMD correctly for very broad distribution analytes which is widely demonstrated not to be the case.

If k is not a constant independent of i then, and if the measurements are made in a linear concentration range for each oligomer i (i.e., $n_i < n_0$), then

$$S_i = k_i n_i \tag{8.11}$$

where k_i is now a function of the oligomer i for a fixed experimental method: sample preparation, instrument operation, and data analysis.

8.7.1.1 Example for Mixtures of Monodisperse Components

The simplest example of gravimetric quantitation to test mass spectrometer response is to create a mixture of two monodisperse compounds: species 1 as a standard and species 2 as the analyte whose concentration is sought. If there is no systematic bias in

the measurement, then the ratio of S_2/S_1 is directly proportional to the gravimetric mass ratio G_2/G_1, where G_i is defined as the gravimetric mass of each species.

The signal from such a mixture, call it A, is

$$S_A = k_1 n_1 + k_2 n_2 \tag{8.12}$$

The mass moments would be

$$M_{nA}^{grav\_exp} = \frac{(k_1 m_1 n_1 + k_2 m_2 n_2)}{(k_1 n_1 + k_2 n_2)} \tag{8.13}$$

$$M_{wA}^{grav\_exp} = \frac{(k_1 m_1^2 n_1 + k_2 m_2^2 n_2)}{(k_1 m_1 n_1 + k_2 m_2 n_2)} \tag{8.14}$$

The gravimetric mass of species i is

$$G_i = m_i n_i \tag{8.15}$$

Substituting into Eq. (8.14) we get

$$M_{wA}^{grav\_exp} = \frac{(k_1 m_1 G_1 + k_2 m_2 G_2)}{(k_1 G_1 + k_2 G_2)} \tag{8.16}$$

To simplify this let the mass fraction X be

$$X = \frac{G_1}{G_1 + G_2} \tag{8.17}$$

Substituting Eq. (8.17) into Eq. (8.16) and dividing numerator and denominator by $(G_1 + G_2)$ yields

$$M_{wA} = \frac{(k_1 m_1 X + k_2 m_2 (1-X))}{(k_1 X + k_2 (1-X))} = \frac{(m_1 X + \theta m_2 (1-X))}{(X + \theta (1-X))} \tag{8.18}$$

where

$$\theta = \frac{k_2}{k_1} \tag{8.19}$$

In this way, the mass bias in the mass spectrum is reduced to a single metric, θ. θ equals one for an unbiased system. If species 2 is overcounted with respect to species 1, θ will be greater than one, if species 2 is undercounted, θ will be less than one. The further θ is from one the greater the systematic bias in the mass spectrum.

8.7.1.2 Example for Mixtures of Polydisperse Components

For most mixtures encountered, any given oligomer peak in the mass spectrum cannot be assigned exclusively to one or the other component of the mixture. In fact, a given oligomer peak may have contributions from both components in the mixture.

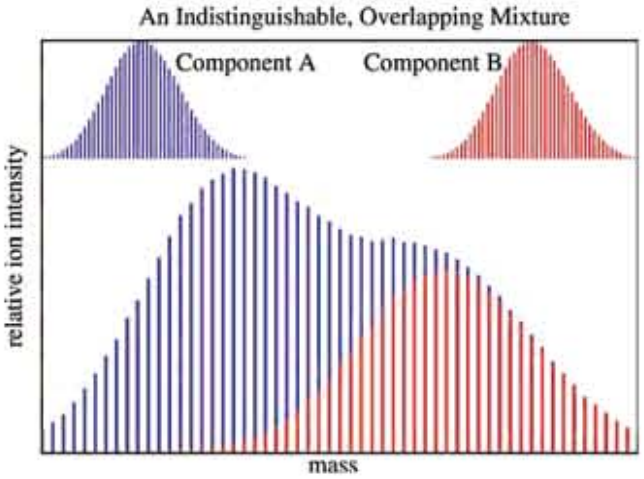

Figure 8.8 Schematic illustration of an indistinguishable and overlapping mixture of two components, where the peak intensities in the mixture are simply sums of component oligomer intensities.

Typically these overlapping MMDs are made up of indistinguishable oligomer components, that is, each component of the mixture has some (but not all) oligomers that are identical to those in the other component as illustrated in Figure 8.8. This means that in this case the mass moments of the mixtures must be calculated and used to create a calibration curve. A full theory for the case of distinguishable oligomer mixtures (shown in Figure 8.9), or nonoverlapping MMDs (shown in Figure 8.10), where each oligomer peak can be assigned to a specific component, is given in Section 8.7.1.5. In this special case, true type B uncertainties can be given for each oligomer in the target material and a true absolute molecular mass standard can be created.

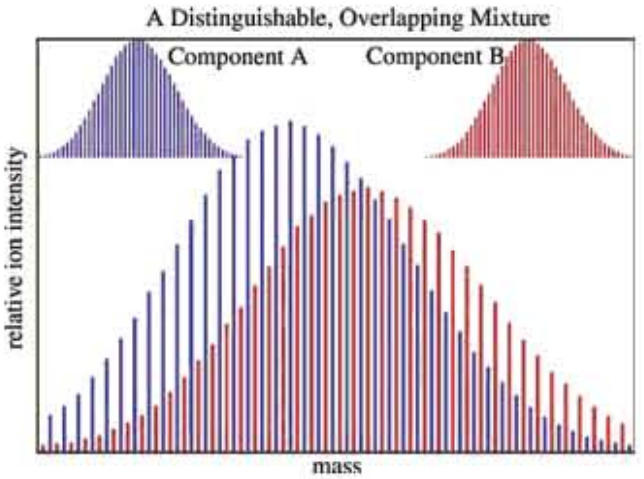

Figure 8.9 Schematic illustration of a distinguishable but overlapping mixture of two components.

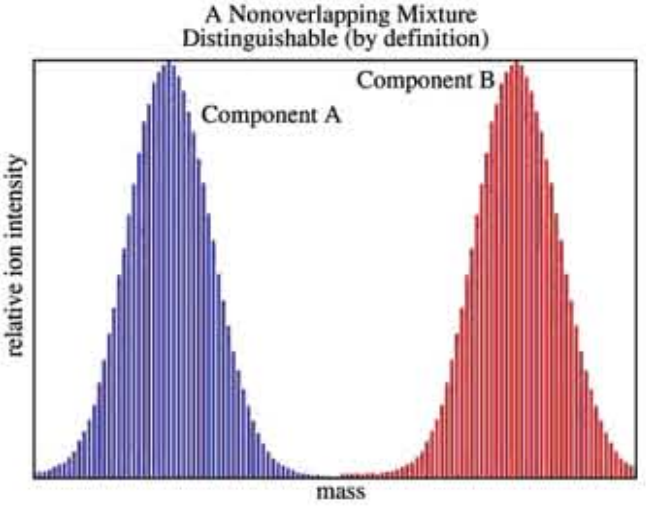

Figure 8.10 Schematic illustration of a nonoverlapping mixture of two components, which is distinguishable by definition.

Equation (8.18) can be extended to a gravimetric mixture of polydisperse components by substituting the experimental average molecular mass of each pure component derived from its mass spectrum. This leads to the mass moments

$$M_{wq}^{\text{grav}} = \frac{(\hat{k}_1 M_{w1}^{\text{exp}} X + \hat{k}_2 M_{w2}^{\text{exp}}(1-X))}{(\hat{k}_1 X + \hat{k}_2(1-X))} = \frac{(M_{w1}^{\text{exp}} X + \theta M_{w2}^{\text{exp}}(1-X))}{(X + \theta(1-X))} \tag{8.20}$$

where q represents a given gravimetric mixture. In Eq. (8.20), $\hat{k}_1$ and $\hat{k}_2$ replace k_1 and k_2 used in the monodisperse example and are the mass-average means over each component of the mixture which is conceptually similar to the mass-average molecular mass. Likewise, X is now calculated from the gravimetric amounts of each component in the mixture. The mass moments of the pure components are from their mass spectra using Eq. (8.21):

$$M_{wq}^{\text{exp}} = \frac{\sum_i S_{iq} m_i^2}{\sum_i S_{iq} m_i} \tag{8.21}$$

To obtain an estimate of the value of θ, the minimum value of the sum of squares is found. The sum of squares over all mixtures q is expressed as

$$SS_\theta = \sum_q (M_{wq}^{\text{grav}} - M_{wq}^{\text{exp}})^2 \tag{8.22}$$

The simplest way to solve this equation is to insert an arbitrary value for θ (typically $\theta = 1$) and calculate a value for SS_θ then increment θ and recalculate SS_θ. This most basic iterative process will yield an optimal value typically in a few steps and can easily be encoded in spreadsheet software. Recall that values of θ near one indicate systems with little bias in the mass spectrum.

8.7.1.3 Calculating the Correction Factor for Each Oligomer

Once θ has been calculated and found to be near one, the next step in the process is to calculate the various k_i in order to correct the MMD. If the k_i are a smoothly and slowly varying function of i (or m_i), a Taylor expansion on k_i may be made around a mass peak near the center of the MMD, termed M_0. The center is used to assure that the function is changing as little as possible over the entire width of the MMD; however, mathematically, the choice is arbitrary. Thus

$$k_i = k_0 + Q(m_i - M_0) + \text{higher order terms in } m_i \tag{8.23}$$

$$S_i = k_0 n_i + Q(m_i - M_0) n_i + \text{higher order terms in } m_i \tag{8.24}$$

where k_0 and Q are the first two coefficients in the Taylor expansion. They are also functions of all the experimental conditions: the instrument parameters, the sample concentrations, and the sample preparation method. (By k_0, it is not meant the k of the zeroth index oligomer but rather the zeroth derivative of the Taylor expansion). In this way, the entire physics of the experiment is folded into these two coefficients. From these assumptions, and dropping the higher order terms in Eq. (8.24), one can derive the following important relationship:

$$M_{wq}^{\exp} = M_{wq}^{0} \left\{ \frac{1 + (Q/k_0)(PD_{wq} M_{wq}^{0} - M_0)}{1 + (Q/k_0)(M_{wq}^{0} - M_0)} \right\} \tag{8.25}$$

where $M_{wq}^{\exp}$ is the mass spectral mass-average molecular mass for the mixture of analytes given in Eq. (8.21). PD_w is mass average PD (M_z/M_w) and is taken here to be the experimentally measured value ($M_z^{\exp}/M_w^{\exp}$). Equation (8.25) is then solved for M_{wq}^{0} for various values of Q/k_0 at a fixed M_0 chosen as described below for the values of the mixtures described by $q = A, B, C$, and so on, and for the initial components of the mixtures described as $j = 1$ and $j = 2$.

For a gravimetric mixture A, $M_{wA}^{\text{grav\_0}}$ is calculated from the values for the individual components M_{w1}^{0} and M_{w2}^{0} computed for each Q/k_0 using a simple weighted average:

$$M_{wA}^{\text{grav\_0}} = \frac{G_1}{G_1 + G_2} M_{w1}^{0} + \frac{G_2}{G_1 + G_2} M_{w2}^{0} \tag{8.26}$$

where G_1 is the gravimetric mass of component 1 in the mix, and G_2 is similarly defined.

For each Q/k_0, the sum of squares, $SS_{(Q/k_0)}$, is computed as

$$SS_{(Q/k_0)} = \sum_{q} (M_{wq}^{\text{grav\_0}} - M_{wq}^{o})^2 \tag{8.27}$$

where the sum is taken over all measured mixtures. The Q/k_0 which gives the minimum value of the $SS_{(Q/k_0)}$ is then taken as the best fit. As with Eq. (8.22), solution

of Eq. (8.27) required iteration over incremented values of Q/k_0. Dropping the higher order terms and rearranging Eq. (8.24) yields

$$\frac{S_i}{k_0 n_i} = 1 + \frac{Q}{k_0}(m_i - M_0) \tag{8.28}$$

Equation (8.28) shows us how to apply the correction factor Q/k_0 to each oligomer i to arrive at a more reliable measure of the MMD. If Q/k_0 were equal to zero, then the mass spectrum would show no mass bias and $S_i = k_0 n_i$. This would mean that the peak areas are directly proportional to the oligomer concentrations in the sample. If Q/k_0 is nonzero, then mass bias is present. If M_0 is taken at the middle of the distribution being calibrated, then the sign of Q/k_0 along with where the mass m_i of an oligomer i is greater than or less than M_0 determines whether the correction to the ion intensity is positive or negative.

8.7.1.4 Step by Step Procedure for Quantitation

The steps of the method can be summarized as follows:

1) Obtain at least two samples having different MMDs but with otherwise very similar, if not identical, properties.

   For example, these could be polymers with different degrees of polymerization or nanoparticles with different levels of functionalization. The different samples could be obtained directly by synthesis or by separation of a single broader molecular mass sample. Two samples are required at a minimum, but additional samples will allow for more calibration points. If possible the only difference between the two should be molecular mass. Any other differences, for example, different functional groups may contribute to mass bias in an uncontrolled way.

2) Take mass spectra of each sample endeavoring to keep all experimental conditions constant.

   As much as possible keep all aspects of the measurement constant. This includes sample preparation, instrument settings, and data analysis. Also, measurements should be made contemporaneously to keep any variables that change over time constant. These variables could be sample preparation conditions, for example, water absorption into samples or solvents, or time drift in instrument settings.

3) Use a laboratory balance to make carefully controlled gravimetric mixtures of two samples in several well-spaced ratios.

   The balance needs to be calibrated and accurate to about least 0.1% of the total mass measured. Any gravimetric errors are carried through the entire analysis. Making stock solutions and then mixing solution volumes can be more accurate than repeated weighing of small amounts of material. Generally, as a practical matter, final weights must be at least 25 mg.

4) Take mass spectra of each mixture using the same experimental conditions as used for the pure components.

   The instrument settings may not be optimal for the mixtures, but they must be held constant to satisfy the self consistency of the method. If the experimental

conditions are such that some oligomers of the mixture have disappeared (as compared to the pure component measurements), then compromise experimental conditions must be found. If this occurs, then it suggests strong mass bias in the measurement.

5) From the mass spectra, calculate the mass-average molecular masses of the pure components and of the mixtures.

   Be careful in the application of "black box" software for this step. Unseen algorithms for data processing can lead to substantial errors in converting the mass spectrum to a MMD. Smoothing can introduce mass bias into a spectrum that is not a product of the measurement itself but of the data analysis method applied.

6) Use Eq. (8.22) to iteratively calculate the minimum value of SS_θ at a given θ.

   The most direct way to do this is to set up a simple spread sheet. Start with $\theta = 1$ and change it systematically by small steps until a minimum in SS_θ is found. If θ is between 0.5 and 2 then the possibility exists that the MMD can be corrected. If not, the results should be treated with caution, and the error is too great to be corrected using only the linear term in the Taylor expansion. See Ref. [104] for an example of computer code to make this calculation.

7) Choose M_0, a mass near the center of the average molecular masses of the two components.

   The exact choice of M_0 is not critical; however, the correction to the distribution will be more accurate near M_0 and less accurate the farther any given oligomer mass is from M_0. If a certain mass range is more critical, then choose M_0 at the center of that range.

8) Use Eq. (8.27) to iteratively calculate the minimum value of $SS_{(Q/k0)}$ at a given Q/k_0.

   Again see Ref. [104] for computational assistance.

9) Use Eq. (8.28) and the value for Q/k_0 to correct the ion intensities S_i in the mass spectrum to arrive at a new MMD.

   Individual oligomer intensities may increase or decrease depending on whether they were undercounted or overcounted in the mass spectrum.

At this stage, the analyst should have a good feel for the degree of mass bias in the mass spectra. Furthermore, if this bias is not too large it can be corrected using the methods outlined in this section. If the bias is large, higher order terms in Eqs. (8.23) and (8.24) need to invoked; however, methods to determine the values of the higher order coefficients have not been created. This is a fruitful topic for future research.

8.7.1.5 Determination of the Absolute MMD

The procedures outlined in this section do not provide systematic uncertainties for the corrected values. The corrected mass spectrum is closer to the true MMD, but just how close is it? In order to determine this, the following procedures must be invoked. These procedures require distinguishable or nonoverlapping mixtures as well as numerical instrument optimization to determine the systematic uncertainties inherent in the instrument. This requires extra effort on the part of the analyst, but an

MMD with both type A (random) and type B (systematic) uncertainties is a very useful calibration standard for MS and any other molecular mass measurement technique.

Starting with Eq. (8.11), $S_i = k_i n_i$, if an assumption is made that k_i is a slowly varying function of i (hence also of m_i), then a Taylor expansion around a mass peak near the center of the MMD, termed M_0, can be made. The center of the mass spectrum is used to assure that the function is changing as little as possible over the entire width of the MMD. Then

$$S_i = k_0 n_i + Q(m_i - M_0)n_i + \text{higher order terms in } m_i \tag{8.29}$$

Here Q and k_0 are functions of M_0 as well as of all the experimental conditions: the instrument parameters, the sample concentrations, and the sample preparation method. (By k_0, it is not meant the k of the zeroth index oligomer but rather the zeroth derivative of the Taylor expansion). In the experimental procedures referred to later, once the instrument parameters and experimental preparation methods are optimized, every attempt was made to keep them constant to insure experimental reproducibility. (Later it will be shown how variation in the machine parameters can affect the variation of Q/k_0 and thus the type B uncertainty.)

The implications of the model embodied in Eq. (8.29) will now be explored and it will be shown how small linear shifts of the calibration constant Q over limited mass ranges effect quantities derivable from mass spectral data. First the total signal, the total detected mass, and the mass ratios of mixtures will be considered, and it will be shown how these quantities relate to the true MMD of the analyte.

The total signal, S_T, from the polymer is given by

$$S_T = \sum_i S_i = k_0 \sum n_i + Q(M_n^0 - M_0) \sum_i n_i \tag{8.30}$$

while the total mass of polymer detected, G_T^{exp}, is given by

$$G_T^{exp} = \sum_i m_i S_i = k_0 M_n^0 \sum_i n_i + Q M_n^0 (M_w^0 - M_0) \sum_i n_i \tag{8.31}$$

where M_n^0 and M_w^0 are defined in Eqs. (8.32) and (8.33), respectively, and are the true number average and mass average relative molecular masses.

$$M_n^0 = \frac{\sum_i m_i n_i}{\sum_i n_i} \tag{8.32}$$

$$M_w^0 = \frac{\sum_i m_i^2 n_i}{\sum_i m_i n_i} \tag{8.33}$$

$$PD_n^0 = \frac{M_w}{M_n} \tag{8.34}$$

$$M_z^0 = \frac{\sum_i m_i^3 n_i}{\sum_i m_i^2 n_i} \tag{8.35}$$

$$PD_w^0 = \frac{M_z}{M_w} \tag{8.36}$$

where m_i is the mass of a discrete oligomer, and n_i is the number of molecules at the given mass m_i. The experimental moments from mass spectrum are defined as M_n, M_w, and M_z, while the true values are given as M_n^0, M_w^0, and M_z^0. PD_n defines the PD index that is a measure of the breadth of the polymer distribution. When PD_n is equal to one (i.e., in statistical terms the variance of MMD is zero), all of the polymer molecules in a sample are of the same molecular mass and the polymer is referred to as monodisperse.

Multiplying Eqs. (8.32) and (8.33) together gives

$$M_w^0 M_n^0 = \frac{\sum_i m_i^2 n_i}{\sum_i n_i} \tag{8.37}$$

Then taking the ratio of Eqs. (8.30) and (8.31), one obtains

$$M_n^{exp} = \frac{\sum m_i S_i}{\sum S_i} \tag{8.38}$$

with the result that

$$M_n^{exp} = M_n^0 \left\{ \frac{(1+(Q/k_0)(M_w^0 - M_0)}{(1+(Q/k_0)(M_n^0 - M_0)} \right\} \tag{8.39}$$

where M_n^{exp} is the experimentally measured M_n^0.

For use later in this section by the same algebra is obtained:

$$M_w^{exp} = \frac{\sum m_i^2 S_i}{\sum m_i S_i} \tag{8.40}$$

with the result that

$$M_w^{exp} = M_w^0 \left\{ \frac{(1+(Q/k_0)(M_z^0 - M_0))}{(1+(Q/k_0)(M_w^0 - M_0))} \right\} \tag{8.41}$$

All higher moments may be obtained in a similar way and have a similar form.

Equation (8.41) gives by simple division:

$$M_w^0 = M_w^{exp} \left\{ \frac{1+(Q/k_0)(M_w^0 - M_0)}{1+(Q/k_0)(M_z^0 - M_0)} \right\} \tag{8.42}$$

which yields

$$M_w^0 = M_w^{exp} \left\{ 1 - \frac{(Q/k_0) M_w^0 (PD_w - 1)}{1+(Q/k_0)(M_z^0 - M_0)} \right\} \tag{8.43}$$

Equation (8.43) states that the deviation of the mass moment measured by mass spectrum from the true mass moment is a function of the PD (arising from that moment) divided by a correction term arising from how far that moment is from

the mass M_0 around which the Taylor expansion to obtain k_0 and Q is centered. In Eq. (8.43), the reader should notice that if M_z^0 is close to M_0 the term in $(Q/k_0)(M_z^0 - M_0)$ is small compared to 1 and the result depends only on the PD of the polymer.

Since the method depends on gravimetrically mixing analytes to obtain estimates of Q/k_0, it is necessary to consider the equations relating to these mixtures. Equation (8.31) states that the MS-measured total mass, G_T^{exp}, is proportional to the true mass, G_T^0:

$$G_T^0 = M_n \sum n_i \tag{8.44}$$

$$G_T^{exp} = k_0 G_T^0 \{1 + Q/k_0(M_w^0 - M_0)\} \tag{8.45}$$

Consider now a mixture of the chemically identical analytes with functional groups having different masses, or two different molecular mass analytes having distributions that are well separated, such that each oligomer in the mass spectrum can be assigned to a specific polymer in the mixture. Call them analyte A and analyte B that will make up the components of the gravimetric mixtures. Then the measured ratio of the masses of each is given by

$$\frac{G_{TA}^{exp}}{G_{TB}^{exp}} = \frac{k_{0A} G_{TA}^0}{k_{0B} G_{TB}^0} \left\{ \frac{1 + (Q_A/k_{0A})(M_{wA}^0 - M_0)}{1 + (Q_B/k_{0B})(M_{wB}^0 - M_0)} \right\} \tag{8.46}$$

Note that the expansions are performed for both polymer distributions A and B around the same M_0. Also note Q_A, Q_B, k_{0A}, and k_{0B} are all functions of M_0. Thus, from Eq. (8.46):

$$\frac{G_{TA}^{exp}}{G_{TB}^{exp}} = \frac{G_{TA}^0}{G_{TB}^0} \left\{ \frac{1 + (Q/k_0)(M_{wA}^0 - M_0)}{1 + (Q/k_0)(M_{wB}^0 - M_0)} \right\} \tag{8.47}$$

Simple algebra leads us to

$$\frac{G_{TA}^{exp}}{G_{TB}^{exp}} = \frac{G_{TA}^0}{G_{TB}^0} \left\{ 1 + \frac{(Q/k_0)(M_{wA}^0 - M_{wB}^0)}{1 + (Q/k_0)(M_{wB}^0 - M_0)} \right\} \tag{8.48}$$

What is measured are $G_{TA}^{exp}/G_{TB}^{exp}$ from MS versus G_{TA}^0/G_{TB}^0 gravimetrically determined. The calculated slope is

$$\text{slope} = \left\{ 1 + \frac{(Q/k_0)(M_{wA}^0 - M_{wB}^0)}{1 + (Q/k_0)(M_{wB}^0 - M_0)} \right\} \tag{8.49}$$

As before with Eq. (8.45), the reader should notice if M_{wB}^0 is close to M_0, the term in $(Q/k_0)(M_{wB}^0 - M_0)$ is small compared to 1 which means the slope depends only on the difference $(M_{wA}^0 - M_{wB}^0)$ and, thus, (Q/k_0) maybe easily calculated. Finally, remember that the gravimetric calibration of the signal axis using chemically identical analytes

can avoid the issues pertaining to the uncertainties arising from ablation, ionization, and detection. However, uncertainties in sample preparation as well as data analysis repeatability and consistency still affect the gravimetric calibration techniques.

8.7.2 Quantitative MMD Measurement by SEC/ESI-MS

Today, SEC is used as the method of choice for the determination of MMDs. The method suffers a number of significant drawbacks. First, it requires calibration with polymer standards whose molecular weights need to be determined by independent techniques [107]. For many polymer classes, well-characterized standards are not available. In these cases, universal calibration, heavily relying on the accuracy of Mark-Houwink parameters and the validity of the Flory-Fox equation [108–112] or, alternatively, online calibration by light scattering and viscosimetric detection have to be employed, which can lead to errors in the MMD of up to 30% [100]. Chromatographic band-broadening further deteriorates the SEC results, with an especially strong impact on the apparent MMD of polymers exhibiting sharp peaks or shoulders as in the case of distributions derived by experiments aimed at the determination of kinetic rate constants [113, 114].

8.7.2.1 Exact Measurement of the MMD of Homopolymers

Barner-Kowollik and coworkers have recently shown that by employing SEC with online concentration detection and using ESI-MS for an internal mass calibration, very accurate MMDs of synthetic polymers can be determined [102]. In the employed chromatographic setup [115, 116] (see Figure 8.11), a concentration-sensitive RI detector and the electrospray mass spectrometer are coupled to the chromatographic effluent of a size-exclusion column in parallel.

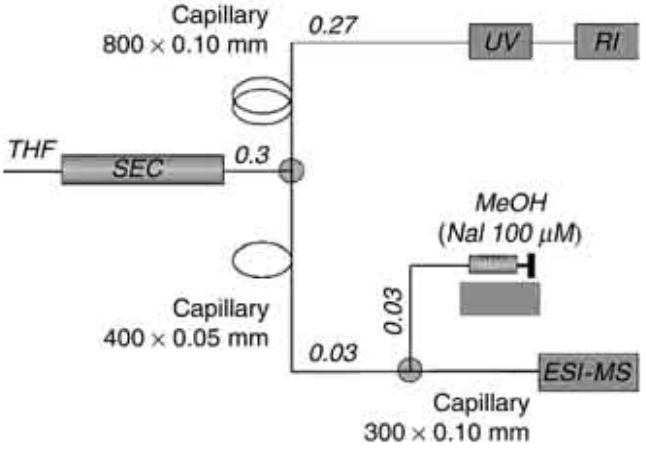

Figure 8.11 Chromatographic setup employed for coupling the concentration-sensitive RI- and/or UV detectors and the ESI-MS to the effluent of an SEC column in parallel. Numbers indicate flow rates in milliliters per minute.

The method accounts for the individual strengths and limitations of both detectors by deriving the absolute polymer concentration solely from the RI-detector trace. The electrospray mass spectrometer is used only in its ability to accurately measure the concentration profiles of the individual oligomers eluting from the chromatographic system for further processing. No use is made of MS to derive absolute concentration data. The elution profiles of the individual oligomers derived by MS contain accurate retention time information. This allows for a precise calibration of the SEC retention time dependence on chain length. A calibration can be derived without additional knowledge of the polymer class or any other physical assumptions as long as the polymer molecule is compatible with ESI. In addition to the position in time, the exact shape of the elution profile can be derived from online ESI-MS, which allows the characterization of the chromatographic band-broadening function as well as corrections to be made for band-broadening effects in the derived MWDs.

The influence of chromatographic band broadening is described mathematically by the discrete form of Tung's convolution equation (8.50) [117]. The SEC-trace, S_{V_R} recorded by a detector with a linear mass concentration response (RI detector) is derived by the convolution of the mass-weighted MMD w_n with the instrumental spread and calibration function, $G_{V_R,n}$. Here V_R and n are the chromatographic retention volume and the polymer repeat unit number, respectively.

$$\mathbf{S} = \mathbf{G} \times \mathbf{w} \quad \text{or} \quad S_{V_R} = \sum_n G_{V_R,n} \cdot w_n \tag{8.50}$$

Figure 8.12 provides a graphical representation of the process described by Eq. (8.50): The individual elution profiles of each oligomer of a certain chain length – instead of being negligibly narrow spikes or delta peaks – feature a somewhat Gaussian peak shape. The RI-detector trace is obtained by a summation over the elution profiles of all individual oligomers, weighted by their respective concentrations. A band-broadened size-exclusion chromatogram is hence much like a blurred picture, where the detailed patterns are partially hidden, as each pixel is smeared out over a larger area determined by the point spread function of the out-of-focus lens.

If the functional form of $G_{V_R,n}$ is known, a number of deconvolution approaches may be applied to derive the reconstructed MMD, $\hat{w}_n$. Unfortunately inversion of

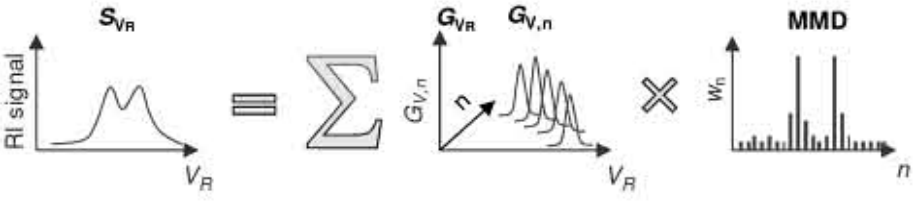

Figure 8.12 Graphical representation of the convolution process in SEC. The concentration of each individual oligomer molecule in the molecular mass distribution is multiplied with its elution profile stored in the instrumental calibration and broadening matrix $G_{V_R,n}$. The individual weighted oligomer profiles are summed to result in the recorded RI-detector trace.

Eq. (8.50) is an "ill-conditioned" problem and direct solution of the convolution equation, for example, by linear regression leads to an amplification of instrumental noise resulting in a highly oscillatory behavior of $\hat{w}_n$ with possibly negative values, lacking physical significance [118, 119]. Sophisticated numerical approaches therefore have to be used for the inversion of (8.50). Today the most widely used and most effective deconvolution approaches are based on singular value filtering and the application of regularization filters [119, 120]. Maximum entropy (MaxEnt) regularization has been successful in a number of related scientific problems in image reconstruction [121, 122] and spectroscopy [123]. It has been argued that use of the Shannon entropy [124] criterion as information constraint is the only consistent way of restoring a probability density function from noisy data [125, 126].

As can be seen in Figure 8.13, online ESI-MS can be used to extract the chromatographic elution profiles of individual oligomers and thus to gain calibration data (retention volume vs. chain length) together with band-broadening information for each individual eluting oligomer. This data can in turn be used to construct $G_{V_R,n}$ without the need for additional information, as long as the extracted ion chromatograms provide a correct representation of the actual elution profiles. Deconvolution of Eq. (8.50) will directly yield the absolutely calibrated MMD, corrected for chromatographic band-broadening effects. In our approach, a MaxEnt-based algorithm was employed in order to compute $\hat{w}_n$. At the heart of this approach lies a constrained nonlinear optimization problem (8.51). The general derivation of the objective function based on Bayesian probability theory can be found elsewhere [127]. The employed algorithm proceeds by calculating the theoretical RI-detector trace from a trial MMD. This concentration trace is then compared against the measured RI-detector trace. The software iteratively manipulates w to obtain the closest possible fit to the measured trace. The total squared sum of error (χ^2) is used to assess the agreement between the measured and the theoretical mass concentration trace. In a typical least squares approach, the single objective would be to minimize χ^2, yielding $\hat{w}_n$ as the maximum likelihood estimator of the MMD. However, as mentioned

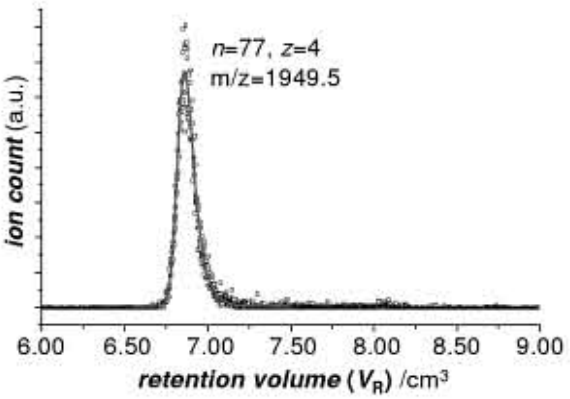

Figure 8.13 Extracted ion chromatogram recorded at $m/z = 1949.5$ Th, effectively reproducing to the elution curve of a hydrogen-functional MMA oligomer of chain length, $n = 77$ in charge state, $z = 4$ (dots), together with a fitted EMG peak profile (grey curve).

before, such an approach would lead to an excessive amplification of noise from the RI-detector trace because in SEC the individual oligomers elute very closely to each other in time, so that many individual elution profiles overlap. This feature of SEC complicates an accurate calculation of the individual contribution of each oligomer to the RI-detector trace and leads to great covariance of the oligomer concentrations in the obtained MMD. The problem is alleviated if a regularization filter – in the current case MaxEnt regularization – is imposed on the estimated MMD [119]. An additional entropy term, S [124–126], introduced in the objective function by means of a Lagrange multiplier, λ ascertains that the MMD $\hat{w}_n$ is as smooth as permitted by some limiting criterion [127]. Nonnegativity constraints in $\hat{w}_n$ and first-order equality constraints of the total area of $\hat{w}_n$ and S_{V_R} can further stabilize deconvolution. Quadratic or Thikonov regularization employing these constraints also yields very good results, while the resulting quadratic optimization problem is less complicated to solve algorithmically.

$$\hat{w}_n = \arg\max_{w}(Q - \lambda \cdot \chi^2) \quad \text{with} \quad w_n > 0 \quad \forall \quad n \tag{8.51}$$

$$\chi^2 = \sum_{V_R} \frac{(S_{V_R,\exp} - \sum_n G_{V_R,n} w_n)^2}{\sigma^2} \tag{8.52}$$

$$Q = \sum_n w_n \cdot \log(w_n) \tag{8.53}$$

Figure 8.14 shows the deconvoluted absolute MMD and the chromatographic peak parameters for a narrow-molecular weight PMMA standard, having a manufacturer-

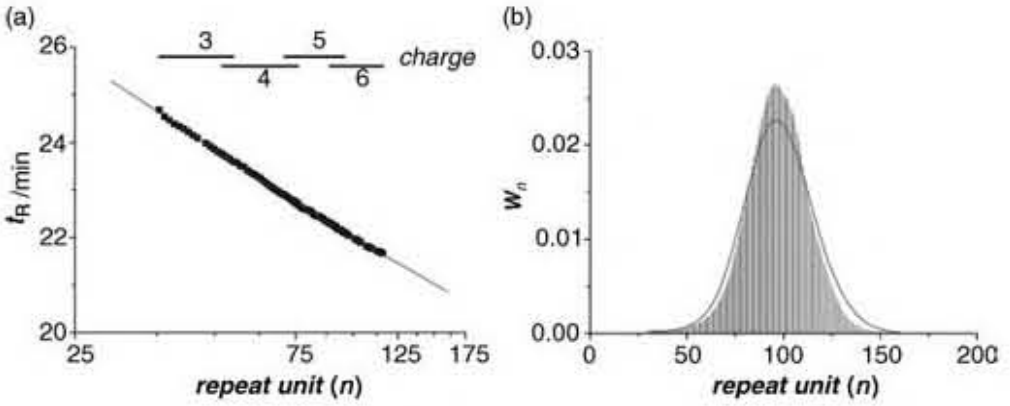

Figure 8.14 (a) SEC retention time (t_R) as a function of the repeat unit length of a narrow PMMA standard with manufacturer-specified $DP_w = 102$, as derived from online ESI-MS (symbols). As can be seen, there is an excellent overlap of the calibration data determined from chromatographic peaks recorded in different charge states. (b) Deconvoluted molecular mass distribution $\hat{w}_n$ obtained from MaxEnt data processing (sticks) and molecular mass distribution obtained from conventional calibration using MS retention time data (curve).

specified weight-averaged degree of polymerization (DP_w) of 102 and polydispersity index (PDI) of 1.03. Linear retention time data free from outliers was obtained for this sample (see Figure 8.14a). In many cases, ions of adjacent charge state appear in the mass spectrum for oligomers of the same chain length. Peak data were extracted for both charge states in these cases and the data is superimposed in Figure 8.14. There was excellent agreement between retention volume data from different charge states as was previously reported by Simonsick *et al.* [115]. Furthermore, for repeat units corresponding to the concentration apex of the MMD, no concentration-induced bias in the retention times is seen for the analyzed sample.

A comparison of the deconvoluted MMD with that obtained from a conventional calibration approach converting the retention volume axis to a molecular weight axis by using only the retention time information without band-broadening correction (Figure 8.14b, red curve) shows that for these narrow standards, the MaxEnt procedure can effectively account for chromatographic band broadening. As can be taken from, molecular weight moments for this standard obtained from SEC/ESI-MS are about 5% lower than specified by the manufacturer and determined using SEC calibrations which can be traced back to light-scattering measurements as absolute calibration source. The number-averaged degree of polymerization of the 10 kg mol^{-1} PMMA standard was calculated independently using ^{1}H-NMR. This technique is an absolute, calibration-free means of determining DP_n. From three consecutive measurements, a $DP_n = 94.5 \pm 1\%$ was calculated, which agrees with the average value obtained by SEC/ESI-MS ($DP_n = 93.4$) within its standard deviation.

8.7.2.2 MMD of the Individual Components in Mixtures of Functional Homopolymers

The great potential of MS in polymer analysis lies in its ability to measure the molecular weight of individual oligomer molecules with an accuracy that allows both the unambiguous identification of the chemical identity of the polymer and its end-groups, as well as an accurate molecular mass calibration of the SEC system. This strength of MS can be used to elucidate the individual MMDs and absolute concentrations of components in mixtures of functional homopolymers. Knowing the identity of the individual polymer species together with their concentrations provides both the synthetic chemist and the polymer kineticist with new toolsets for the characterization and optimization of polymerization processes.

The current approach features a direct extension of the method of absolute molecular weight derivation for pure polymers (described in Section 8.7.2.1) [102] to mixtures of individual polymer species [103]. An assumption is made that ESI-MS can be used to successfully derive the relative concentrations of polymers eluting from the SEC-column, as long as they are of the same chain length. In other words, it is assumed that there is no significant end-group bias on ionization efficiency. Furthermore, it is assumed that influences of the polymer end groups and the chain length of the polymer on the RI increment, dn/dc are negligible. As demonstrated by a number of authors, this assumption is generally valid except for low-molecular weight oligomers of less than about 20 repeat units [128–130].

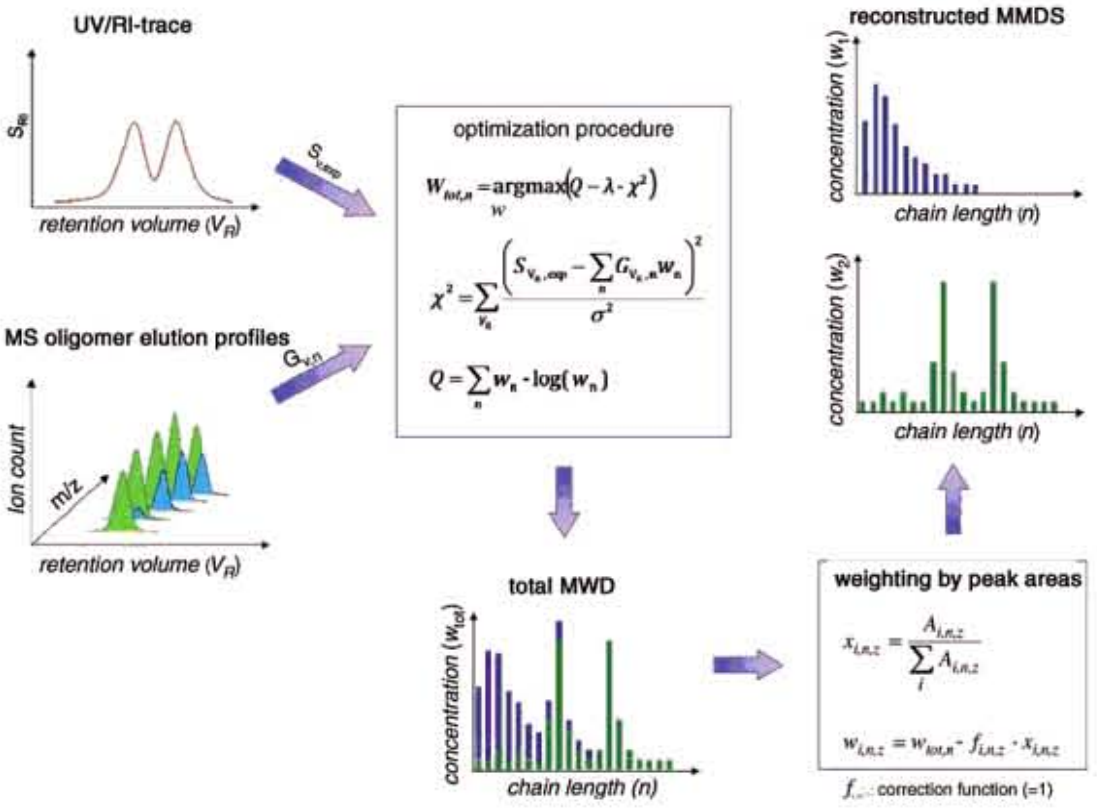

Figure 8.15 Flow diagram of the principal data processing approach. The instrumental calibration and band-broadening matrix $G_{V,n}$ derived by online mass spectrometry as well as the RI-detector trace $S_{V,exp}$ are processed to arrive at the deconvoluted total molecular mass distributions w_{tot}. Weighting of w_{tot} by the areas under the peaks of the individual functional oligomers $A_{i,n,z}$ yields w_i.

The MMD of a single species $\hat{w}_{i,n,z}$ is thus calculated by simply weighting the net MMD $\hat{w}_n$ with the ratio $x_{i,n,z}$ of the areas under the individual functional oligomer peaks, $A_{i,n,z}$ of the species to the total area of all functional oligomer elution profiles at the fixed charge state z and repeat unit number n (see Figure 8.15 – "weighting by peak areas").

$$\hat{w}_{i,n,z} = \hat{w}_n \cdot f_{i,n,z} \cdot x_{i,n,z} \quad \text{with} \quad x_{i,n,z} = \frac{A_{i,n,z}}{\sum_i A_{i,n,z}} \tag{8.15}$$

This approach is possible even in the presence of strong molecular mass influences on the ionization efficiency, as a quantitative rationing is carried out only between the abundance of different end-group-carrying polymers of the same repeat unit. Such a methodology is feasible as long as there is only a negligible effect of the end group on ionization efficiency in the electrospray source. Furthermore, all species with the same repeat unit need to arrive at the mass spectrometer at the same retention time, so that ionization occurs in the same chemical background. The latter assumption is valid in most cases, as the influence of the end group on hydrodynamic

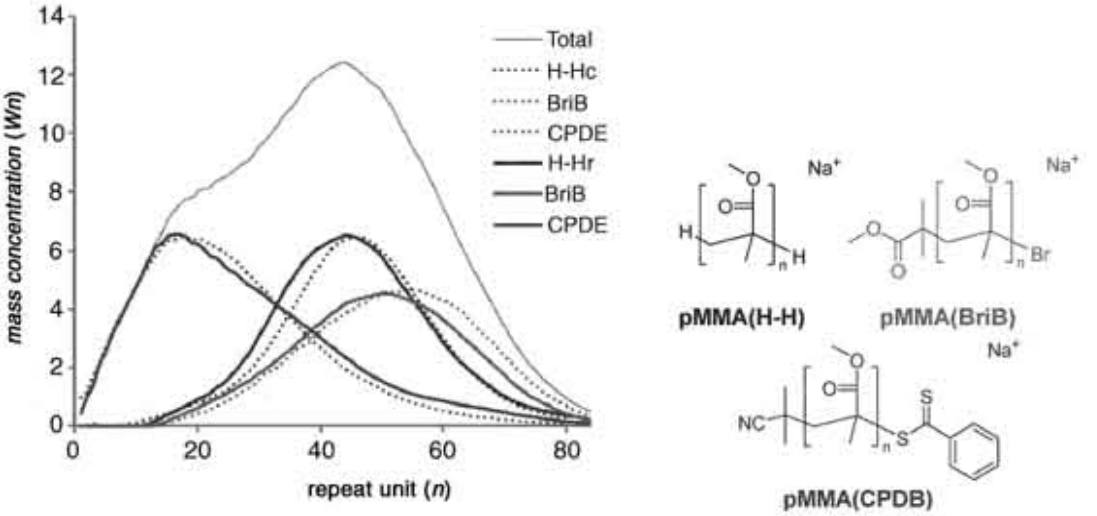

Figure 8.16 Reconstructed and original mass-weighted molecular mass distributions for a ternary $1:1:1_w$ mixture of hydrogen-functional (H-H), bromine-functional (BriB), and dithiobenzoate functional (CPDB) PMMA.

volume is typically negligible when compared to the polymer backbone. To account for possible end-group bias, a correction factor $f_{i,n,z}$ may be introduced. Because of a lack of a proper functional description of the ionization process, negligible end-group influences were assumed in the current approach ($f \equiv 1$). A validation of this assumption as well as of the general applicability of the proposed method is given in the following paragraph.

Three functional polymer species were used to validate the developed method (see Figure 8.16): Commercial standards of PMMA synthesized by anionic group transfer polymerization and carrying only hydrogen as end group are denoted by PMMA (H-H). These standards were mixed in different weight ratios with PMMA synthesized by atom transfer radical polymerization carrying a bromine end group denoted by PMMA(BriB) and PMMA(CPDB) synthesized by cyanoisopropyl dithiobenzoate-mediated reversible addition fragmentation chain transfer polymerization.

The original molecular weight distributions of each species together with the reconstructions from a $1:1:1_w$ mixture of these species are given in Figure 8.16. Generally, a good agreement was attained between the individual original molecular weight distributions and those that were reconstructed. The average degrees of polymerization of PMMA(CPDB) are overestimated by around 8%, whereas the degrees of polymerization of PMMA(H-H) and PMMA(BriB) are underestimated by around 2% and 5%, respectively. Agreement between the original and reconstructed area under the distribution (total mass concentration) is better, featuring a maximum deviation of 5%.

The roughly 5% lower molecular weight averages of the original distribution of PMMA(H-H) compared to the manufacturer-stated values are in agreement with earlier findings. Any systematic error in the reconstructed molecular weights is likely to be due to resolution limitations of the mass analyzer toward higher molecular weights, as well

as to possible unrecognized side products in the polymer standards and adduct formation with salt and solvents. Baseline subtraction in the oligomer peak elution proved to be difficult in some cases, due to background suppression and unresolved peaks, thereby influencing correct calculation of the peak area ratios. The accuracy of the current method especially in cases where there are only minor amounts of one species present in a mixture can be improved. Proper baseline correction and safeguards against mass spectral overlap are thus important issues to be addressed in further investigations, in order to further extent the dynamic range and mass range of the method.

8.7.3
Comparison of the Two Methods for MMD Calculation

The methods presented in Sections 8.7.1 and 8.7.2 – although being based on two conceptually very different approaches – provide for the first time a means to measure the MMD of synthetic polymers with unrivaled accuracy. In the accessible molecular weight range of up to several tens of kilograms per mole, depending on instrumental resolution, these methods therefore pose serious alternatives for the molecular mass measurement of synthetic polymers by MS.

The typical areas of application of each method should be noted: The method based on MALDI-MS with internal calibration together with a very thorough error analysis developed at the NIST provides for the first time a tool to generate truly accurate molecular mass standards where the molecular mass uncertainties can be ultimately traced back to basic gravimetric and volumetric measurements. The polystyrene MMD standard, SRM 2881 is the final product of this effort. The method furthermore allows quantitative assessment of the mass bias observed in polymer analysis not just by MALDI-MS but by chromatographic and other methods as well. The determination of the absolute MMD opens the door for many experiments where the shape of the MMD plays a critical role in polymer behavior as in viscosity and rheology.

In the SEC/ESI-MS method on the other hand, a characterization of the molecular mass bias is not attempted or deemed possible. The method relies on the online internal molecular mass calibration of SEC, using MS only in its potential to determine the molecular weight and elution times of macromolecules with high accuracy and regardless of the polymer chemical identity as long as ionization can be achieved. Any data on the concentration of macromolecules eluting from the SEC column is obtained from a concentration-sensitive detector (an RI detector in the current case). Although relying on a couple of assumptions, this method is deemed to be especially useful when fast but at the same time accurate determinations of MMDs and compositions are required of many polymer species of differing chemical makeup (e.g., in an industrial laboratory setting or in high-throughput experimentation).

The availability of these two methods, which each rely on physically very different approaches to ultimately provide the same molecular mass information, allows an assessment of their accuracy by direct comparison. Figure 8.17 shows the number fraction of styrene oligomers against repeat unit length for SRM 2881, as determined by the NIST MALDI-based method (circles with 95% confidence interval) [101] and by

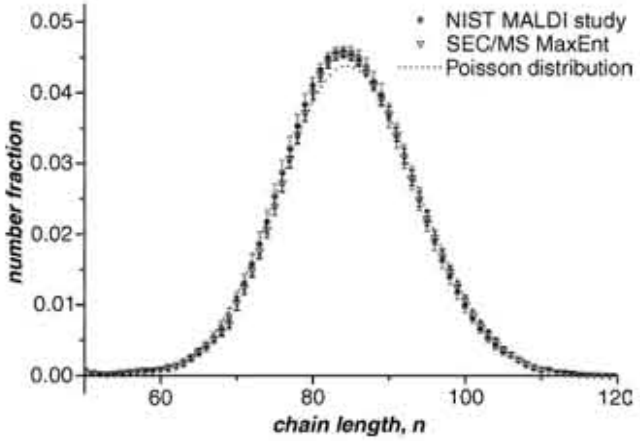

Figure 8.17 The MMD of the NIST polystyrene molecular mass standard SRM 2881. The NIST-certified number fractions (circles) were determined by MALDI-MS using an internal calibration procedure of the mass spectrometric intensity axis [101]. A comparison with the MMD determined by an SEC/ESI-MS analysis with data treatment by the MaxEnt method (triangles) [102] reveals the excellent agreement between the molecular mass data obtained from these two, conceptually very different methods.

a triple repeat measurement of the same standard employing SEC/ESI-MS (triangles) with ionization by $AgBF_4$ [102].[3)] The excellent agreement of the MMDs serves as proof of the high accuracy of molecular mass data obtained from each of these two methods. This is further supported by an independent measurement of DP_n by ^{1}H-NMR in the case of the SEC/ESI-MS approach [102].

8.7.4
Simple Methods for the Determination of the Molar Abundance of Functional Polymers in Mixtures

The above described methods have highlighted approaches that can be employed – via the online coupling of SEC and ESI-MS – to arrive at exact mass distributions of components (i.e., individual chain termini differentiated chains) of homo- and copolymers, allowing for the extraction of absolute concentrations of individual chains. While these approaches are – in terms of accuracy – very reliable, they are also associated with a considerable instrumental and mathematical complexity. In the following text, a method is presented that allows to quantitatively evaluate mass spectra with regard to individual chain distributions with minimal computational demand, while providing satisfactory results. In an ideal scenario, one would have

3) Note that the error bars of the MALDI-derived MMD are the 95% confidence intervals, based on a careful assessment of all errors including those in sample preparation (weighting, volumetric measurements, and spotting), whereas the SEC/MS 95% confidence intervals are based on a triple repeat measurement of a single standard solution and therefore only reflect repeatability of the analytical data acquisition process.

mass spectra at hand that display no mass bias at all. In reality, however, there may always be a certain amount of mass bias present. Let's assume a scenario where the ratio of two components in a polymer mixture (i.e., two chain distributions with different yet well-defined end groups) is to be quantified (the presented approach can readily be expanded to more components). In the most simple and straightforward approach for quantitatively evaluating mass data, the height of two peaks that do not show isobaric overlap (i.e., P_1 and P_2, the species of interest), Δh^{P1}, is evaluated in each repeat unit. As the height of each nonoverlapping single isotopic peak (alternatively the integral could be employed) is proportional to the number of molecules corresponding to the associated mass, the individual peak heights can be employed to arrive at the mole fraction of one of the species, F, via Eq. (8.55). Note that F is given as $F(i)$, as it can be evaluated in every repeat unit, with i being the chain length to which the repeat unit corresponds.

$$F^{P_1}(i) = \frac{\Delta h^{P_1}(i)}{\Delta h^{P_1}(i) + \Delta h^{P_2}(i)} \tag{8.55}$$

While Eq. (8.55) can be a valuable tool as $F(i) = F$ indicates the absence of mass bias [131], it does not take into account any potential chain length-dependent ionization mass biases other than evaluation of every repeat unit. However, a further refinement allows for the elimination of the mass bias. A useful approach was taken by Günzler *et al.* in previous quantitative mass spectrometric evaluations [132, 133]: Let $G(i)$ be the ratio of the peak heights of P_1 and $P_2 \forall i$. This ratio may directly be plotted against chain length, i, and yields identical information to $F(i)$ as $F(i) = G(i)\cdot(G(i) + 1)^{-1}$. Now define $G'(i,i-1)$, $G''(i,i+1)$ in a similar manner to $G(i)$, however taking the height of $P_2(\Delta h^{P_2})$ from one repeat unit higher (Eq. (8.57)) or lower (Eq. (8.58)). Thus, the vectors $G(i)$, $G'(i,i-1)$, and $G''(i,i+1)$ are obtained.

$$G(i) = \frac{\Delta h^{P_1}(i)}{\Delta h^{P_2}(i)} \tag{8.56}$$

$$G'(i,i-1) = \frac{\Delta h^{P_1}(i)}{\Delta h^{P_2}(i-1)} \tag{8.57}$$

$$G''(i,i+1) = \frac{\Delta h^{P_1}(i)}{\Delta h^{P_2}(i+1)} \tag{8.58}$$

In a subsequent step, $G(i)$, $G'(i,i-1)$, and $G''(i,i+1)$ are individually averaged $\forall i$, yielding the average values $\langle G\rangle$, $\langle G'\rangle$, and $\langle G''\rangle$. $\langle G\rangle$ corresponds to the average ratio within the same repeat unit, $\langle G'\rangle$ corresponds to the average ratio within two repeat units with the second repeat unit being at smaller molecular weights, and $\langle G''\rangle$ corresponds to the average ratio of within two repeat units with the second repeat unit being at larger molecular weights. With $\langle G\rangle$, $\langle G'\rangle$, and $\langle G''\rangle$ at hand, one can plot these values against $\Delta m/z$, that is, the difference in Th between the positions $(i-1)$, i, and $(i+1)$. The y-intercept ($\Delta m/z = 0$) of such a plot yields $\langle G\rangle^{\Delta m/z,0}$, which represents the mass bias free ratio of the two products P_1 and P_2 in the polymer sample. In systems where the mass bias is negligible, all the evaluation procedures,

that is, averaging $F(i)$, $G(i)$, and calculating $\langle G \rangle^{\Delta m/z,0}$ should give (near) identical results, providing a guide toward assessing whether more complex evaluation procedures – as detailed in the previous sections – are required. In a range of systems, the above approach has provided satisfactory results [131–133].

8.8 Conclusions and Outlook

The current chapter has provided an account of the contemporary status of the field of automated MS data processing in synthetic polymer chemistry. Especially in the recent couple of years, some important advances have been made in fields including copolymer compositional characterization, the determination of accurate MMDs, and the automated interpretation and integration of polymer MS data. The increasing use of hyphenated techniques including MS/MS [88, 96, 134–136], IMS [137, 138], and LC-MS [76, 103, 139, 140] lead to the generation of large spectroscopic datasets. The necessity of automated techniques for an efficient processing of these large and information-rich data in MS has been realized at an early point in the related fields of biomacromolecular analysis and proteomics. Fragmentation databases and highly sophisticated automated processing tools form an integral part of the MS-based proteomics today. Trends toward the creation of fragmentation databases to aid the interpretation of MS/MS data are seen also in the polymer analysis community [94, 95, 141], but the amount of freely available software tools is presently very limited, with the only example being Polymerator by Thalassinos *et al.* [95]. It is no question that the coming years will see the development of further sophisticated computational tools to aid the polymer science community. The synergies with biomacromolecular MS should be realized and the already (freely) available software tools [3, 4, 78] should be customized to synthetic polymer applications and further exploited.

References

1 Pedrioli, P.G.A., Eng, J.K., Hubley, R., Vogelzang, M., Deutsch, E.W., Raught, B., Pratt, B., Nilsson, E., Angeletti, R.H., Apweiler, R., Cheung, K., Costello, C.E., Hermjakob, H., Huang, S., Julian, R.K., Kapp, E., McComb, M.E., Oliver, S.G., Omenn, G., Paton, N.W., Simpson, R., Smith, R., Taylor, C.F., Zhu, W., and Aebersold, R. (2004) *Nat. Biotech.*, **22** (11), 1459–1466.

2 Listgarten, J. and Emili, A. (2005) *Mol. Cellular Proteomics*, **4** (4), 419–434.

3 Deutsch, E.W., Mendoza, L., Shteynberg, D., Farrah, T., Lam, H., Tasman, N., Sun, Z., Nilsson, E., Pratt, B., Prazen, B., Eng, J.K., Martin, D.B., Nesvizhskii, A.I., and Aebersold, R. (2010) *PROTEOMICS*, **10** (6), 1150–1159.

4 Deutsch, E.W., Lam, H., and Aebersold, R. (2008) *Physiol. Genomics*, **33** (1), 18–25.

5 Deutsch, E. (2008) *PROTEOMICS*, **8** (14), 2776–2777.

6 Shah, A.R., Davidson, J., Monroe, M.E., Mayampurath, A.M., Danielson, W.F., Shi, Y., Robinson, A.C., Clowers, B.H., Belov, M.E., Anderson, G.A., and Smith, R.D. (2010) *J. Am. Soc. Mass Spectrom.*, **21** (10), 1784–1788.

7 Further information can be found on the internet at http://psidev.info and http://tools.proteomecenter.org (last accessed: 12.12.2010).

8 Wallace, W.E., Guttman, C.M., Flynn, K.M., and Kearsley, A.J. (2007) *Anal. Chim. Acta*, **604** (1), 62–68.

9 Gruendling, T., Hart-Smith, G., Davis, T.P., Stenzel, M.H., and Barner-Kowollik, C. (2008) *Macromolecules*, **41** (6), 1966–1971.

10 Ladavière, C., Lacroix-Desmazes, P., and Delolme, F. (2008) *Macromolecules*, **42** (1), 70–84.

11 Jackson, A.T., Bunn, A., Priestnall, I.M., Borman, C.D., and Irvine, D.J. (2006) *Polymer*, **47**, 1044–1054.

12 Jiang, X., Schoenmakers, P.J., van Dongen, J.L.J., Lou, X., Lima, V., and Brokken-Zijp, J. (2003) *Anal. Chem.*, **75**, 5517–5524.

13 Murgasova, R. and Hercules, D.M. (2002) *Anal. Bioanal. Chem.*, **373**, 481–489.

14 Naidong, W., Chen, Y.-L., Shou, W., and Jiang, X. (2001) *J. Pharm. Biomed. Anal.*, **26**, 753–767.

15 Gemperline, P. (ed.) (2006) *Practical Guide to Chemometrics*, 2nd edn, CRC Press, Boca Raton, FL.

16 Asperger, A., Efer, J., Koal, T., and Engewald, W. (2001) *J. Chromatogr. A*, **937**, 65–72.

17 Sautour, M., Rouget, A., Dentigny, P., Divies, C., and Bensoussan, M. (2001) *J. Appl. Microbiol.*, **91**, 900–906.

18 Tak, V., Kanaujia, P.K., Pardasani, D., Kumar, R., Srivastava, R.K., Gupta, A.K., and Dubey, D.K. (2007) *J. Chromatogr. A*, **1161**, 198–206.

19 Rudaz, S., Cherkaoui, S., Gauvrit, J.-Y., Lantéri, P., and Veuthey, J.-L. (2001) *Electrophoresis*, **22**, 3316–3326.

20 Bateman, K., Seto, C., and Gunter, B. (2002) *J. Am. Soc. Mass. Spectrom.*, **13**, 2–9.

21 Riter, L.S., Vitek, O., Gooding, K.M., Hodge, B.D., and Julian, R.K.J. (2005) *J. Mass Spectrom.*, **40**, 565–579.

22 Knowles, J. (2009) *Computational Intelligence Magazine, IEEE*, **4** (3), 77–91.

23 Vaidyanathan, S., Broadhurst, D.I., Kell, D.B., and Goodacre, R. (2003) *Anal. Chem.*, **75** (23), 6679–6686.

24 O'Hagan, S., Dunn, W.B., Brown, M., Knowles, J.D., and Kell, D.B. (2005) *Anal. Chem.*, **77** (1), 290–303.

25 Wetzel, S.J., Guttman, C.M., Flynn, K.M., and Filliben, J.J. (2006) *J. Am. Soc. Mass Spectrom.*, **17** (2), 246–252.

26 Kelley, C.T. (1999) *Iterative Methods for Optimization*, Society for Industrial and Applied Mathematics, Philadelphia.

27 Spall, J.C. (2003) *Introduction to Stochastic Search and Optimization*, Wiley-Interscience, Hoboken, NJ.

28 Gilmore, P. and Kelley, C.T. (1995) *SIAM J. Optim.*, **5** (2), 269–285.

29 Gruendling, T., Guilhaus, M., and Barner-Kowollik, C. (2009) *Macromol. Rapid Commun.*, **30**, 589–597.

30 Meier, M.A.R., Adams, N., and Schubert, U.S. (2007) *Anal. Chem.*, **79**, 863–869.

31 Brandt, H., Ehmann, T., and Otto, M. (2010) *Anal. Chem.*, **82** (19), 8169–8175.

32 Brandt, H., Ehmann, T., and Otto, M. (2010) *Rapid Commun. Mass Spectrom.*, **24** (16), 2439–2444.

33 Brandt, H., Ehmann, T., and Otto, M. (2010) *J. Am. Soc. Mass Spectrom.*, **21** (11), 1870–1875.

34 Armanino, C. and Forina, M. (1987) *Chemometrics and Species Identification*, vol. **141**, Springer, Berlin.

35 Zupan, J. (1989) *Algorithms for Chemists*, Wiley, New York.

36 Papas, A.N. (1989) *CRC Crit. Rev. Anal. Chem.*, **20** (6), 359–404.

37 Kateman, G. and Buydens, L. (1993) Data processing, in *Quality Control in Analytical Chemistry*, vol. 60, Wiley, New York.

38 Hippe, Z., Bierowska, A., and Pietryga, T. (1980) *Anal. Chim. Acta*, **122**, 279–290.

39 Savitsky, A. and Golay, M.J.E. (1964) *Anal. Chem.*, **36** (8), 1627–1639.

40 Eilers, P.H.C. (2003) *Anal. Chem.*, **75**, 3299–3304.

41 Vivó-Truyols, G. and Schoenmakers, P.J. (2006) *Anal. Chem.*, **78**, 4598–4608.

42 Kast, J., Gentzel, M., Wilm, M., and Richarson, K. (2003) *J. Am. Soc. Mass Spectrom.*, **14**, 766–776.

43 Zhang, P., Li, H., Zhou, X., and Wong, S. (2008) *Int. J. Hybrid Intel. Sys.*, **5**, 197–208.

44 Wiener, N. (1949) *Extrapolation, Interpolation, and Smoothing of Stationary Time Series with Engineering Applications*, Technology Press of MIT & John Wiley, New York.

45 Wallace, W.E. and Guttman, C.M. (2002) J. Res. Nat. Inst. Stand. Tech., **107**, 1–17.

46 Wallace, W.E., Guttman, C.M., and Antonucci, J.M. (1999) *J. Am. Soc. Mass Spectrom.*, **10**, 224–230.

47 Tecklenburg, R.E., Wallace, W.E., and Chen, H. (2001) *Rapid Commun. Mass Spectrom.*, **15**, 2176–2185.

48 Luftmann, H. and Kehr, S. (2007) *e-polymers*, Art. No. 10.

49 Boggs, P.T., Byrd, R.H., and Schnabel, R.B. (1987) *SIAM J. Sci. Stat. Comput.*, **8** (6), 1052–1078.

50 Wallace, W.E., Kearsley, A.J., and Guttman, C.M. (2004) *Anal. Chem.*, **76**, 2446–2452.

51 Barrondale, I. (1968) *Appl. Stat.*, **17**, 51–57.

52 Barrondale, I. and Roberts, F.D.K. (1973) *SIAM J. Numer. Anal.*, **10** (5), 839–848.

53 Duda, R.O. and Hart, P.E. (1973) *Pattern Classification and Scene Analysis*, John Wiley and Sons, Inc., New York.

54 Kearsley, A.J., Wallace, W.E., and Guttman, C.M. (2005) *Appl. Math. Lett.*, **18**, 1412–1417.

55 Kearsley, A.J. (2006) *J. Res. Nat. Inst. Stand. Tech.*, **111** (2), 121–125.

56 Douglas, D.H. and Peucker, T.K. (1973) *Canadian Cartographer*, **10** (2), 112–122.

57 Boggs, P.T., Kearsley, A.J., and Tolle, J.W. (1999) *SIAM J. Opt.*, **9** (3), 755–778.

58 Beyer, W.H. (1981) *CRC Standard Mathematical Tables*, CRC Press, Boca Raton, FL.

59 Montaudo, M.S. (2002) *Mass Spectrom. Rev.*, **21** (2), 108–144.

60 Montaudo, A.S. and Montaudo, G. (1992) *Macromolecules*, **25**, 4264–4280.

61 Montaudo, M.S. and Montaudo, G. (1993) *Makromol. Chem. Makromol. Symp.*, **65**, 269.

62 Zoller, D.L. and Johnston, M.V. (1997) *Anal. Chem.*, **69**, 3791–3795.

63 Willemse, R.X.E., Staal, B.B.P., Donkers, E.H.D., and van Herk, A.M. (2004) *Macromolecules*, **37** (15), 5717–5723.

64 Simonsick, W.J. and Prokai, L. (1995) *Chromatographic Characterization of Polymers* (eds T. Provder, H., Barth and M. Urban), ACS, Washington, DC, p. 41.

65 Nuwaysir, L.M., Wilkins, C.L., and Simonsick, W.J. (1990) *J. Am. Soc. Mass. Spectrom.*, **1**, 66.

66 Montaudo, G., Montaudo, M.S., Scamporrino, E., and Vitalini, D. (1992) *Macromolecules*, **25**, 5099.

67 Wilczek-Vera, G., Yu, Y., Waddell, K., Danis, P.O., and Eisenberg, A. (1999) *Rapid Commun. Mass Spectrom.*, **13** (9), 764–777.

68 Wilczek-Vera, G., Danis, P.O., and Eisenberg, A. (1996) *Macromolecules*, **29** (11), 4036–4044.

69 Wilczek-Vera, G., Yu, Y., Waddell, K., Danis, P.O., and Eisenberg, A. (1999) *Macromolecules*, **32** (7), 2180–2187.

70 Suddaby, K.G., Hunt, K.H., and Haddleton, D.M. (1996) *Macromolecules*, **29** (27), 8642–8649.

71 Willemse, R.X.E. and van Herk, A.M. (2006) *J. Am. Chem. Soc.*, **128** (13), 4471–4480.

72 Huijser, S., Staal, B.B.P., Huang, J., Duchateau, R., and Koning, C.E. (2006) *Biomacromolecules*, **7** (9), 2465–2469.

73 Huijser, S., Staal, B.B.P., Huang, J., Duchateau, R., and Koning, C.E. (2006) *Angew. Chem. Int. Ed.*, **45** (25), 4104–4108.

74 Staal, B.B.P. (2005) *Characterization of (co)polymers by MALDI-TOF-MS*, Technische Universiteit Eindhoven, Eindhoven.

75 Weidner, S.M., Falkenhagen, J., Maltsev, S., Sauerland, V., and Rinken, M. (2007) *Rapid Commun. Mass Spectrom.*, **21** (16), 2750–2758.

76 Weidner, S., Falkenhagen, J., Krueger, R.-P., and Just, U. (2007) *Anal. Chem.*, **79** (13), 4814–4819.

77 Vivó-Truyols, G., Staal, B., and Schoenmakers, P.J. (2010) *J. Chromatogr. A*, **1217** (25), 4150–4159.

78 Aebersold, R. and Mann, M. (2003) *Nature*, **422** (6928), 198–207.

79 Yates, J.R., Ruse, C.I., and Nakorchevsky, A. (2009) *Annu. Rev. Biomed. Eng.*, **11** (1), 49–79.

80 Selby, T.L., Wesdemiotis, C., and Lattimer, R.P. (1994) *J. Am. Soc. Mass Spectrom.*, **5** (12), 1081–1092.

81 Lattimer, R.P. (1994) *J. Am. Soc. Mass Spectrom.*, **5** (12), 1072–1080.

82 Lattimer, R.P. (1992) *J. Am. Soc. Mass Spectrom.*, **3** (3), 225–234.

83 Lattimer, R.P. (1992) *Int. J. Mass Spec. Ion Proc.*, **116** (1), 23–36.

84 Jackson, A.T., Green, M.R., and Bateman, R.H. (2006) *Rapid Commun. Mass Spectrom.*, **20** (23), 3542–3550.

85 Jackson, A.T., Bunn, A., Priestnall, I.M., Borman, C.D., and Irvine, D.J. (2006) *Polymer*, **47** (4), 1044–1054.

86 Jackson, A.T., Scrivens, J.H., Williams, J.P., Baker, E.S., Gidden, J., and Bowers, M.T. (2004) *Int. J. Mass Spectrom.*, **238** (3), 287–297.

87 Jackson, A.T., Slade, S.E., and Scrivens, J.H. (2004) *Int. J. Mass Spectrom.*, **238** (3), 265–277.

88 Jackson, A.T., Bunn, A., Hutchings, L.R., Kiff, F.T., Richards, R.W., Williams, J., Green, M.R., and Bateman, R.H. (2000) *Polymer*, **41** (20), 7437–7450.

89 Borman, C.D., Jackson, A.T., Bunn, A., Cutter, A.L., and Irvine, D.J. (2000) *Polymer*, **41** (15), 6015–6020.

90 Jackson, A.T., Yates, H.T., Scrivens, J.H., Green, M.R., and Bateman, R.H. (1998) *J. Am. Soc. Mass Spectrom.*, **9** (4), 269–274.

91 Scrivens, J.H., Jackson, A.T., Yates, H.T., Green, M.R., Critchley, G., Brown, J., Bateman, R.H., Bowers, M.T., and Gidden, J. (1997) *Int. J. Mass Spectrom. Ion Proc.*, **165–166**, 363–375.

92 Jackson, A.T., Yates, H.T., Scrivens, J.H., Green, M.R., and Bateman, R.H. (1997) *J. Am. Soc. Mass Spectrom.*, **8** (12), 1206–1213.

93 Jackson, A.T., Yates, H.T., Scrivens, J.H., Critchley, G., Brown, J., Green, M.R., and Bateman, R.H. (1996) *Rapid Commun. Mass Spectrom.*, **10** (13), 1668–1674.

94 Baumgaertel, A., Weber, C., Knop, K., Crecelius, A., and Schubert, U.S. (2009) *Rapid Commun. Mass Spectrom.*, **23** (6), 756–762.

95 Thalassinos, K., Jackson, A.T., Williams, J.P., Hilton, G.R., Slade, S.E., and Scrivens, J.H. (2007) *J. Am. Soc. Mass Spectrom.*, **18** (7), 1324–1331.

96 Jackson, A., Slade, S., Thalassinos, K., and Scrivens, J. (2008) *Anal. Bioanal. Chem.*, **392** (4), 643–650.

97 Jackson, A.T., Thalassinos, K., John, R.O., McGuire, N., Freeman, D., and Scrivens, J.H. (2010) *Polymer*, **51** (6), 1418–1424.

98 Karas, M. and Hillenkamp, F. (1988) *Anal. Chem.*, **60** (20), 2299–2301.

99 Fenn, J.B. (2003) *Angew. Chem. Int. Ed.*, **42** (33), 3871–3894.

100 Barner-Kowollik, C., Davis, T.P., and Stenzel, M.H. (2004) *Polymer*, **45**, 7791–7805.

101 Guttman, C.M., Flynn, K.M., Wallace, W.E., and Kearsley, A.J. (2009) *Macromolecules*, **42** (5), 1695–1702.

102 Gruendling, T., Guilhaus, M., and Barner-Kowollik, C. (2008) *Anal. Chem.*, **80**, 6915–6927.

103 Gruendling, T., Guilhaus, M., and Barner-Kowollik, C. (2009) *Macromolecules*, **42** (17), 6366–6374.

104 Wallace, W.E. and Guttman, C.M. (2010) *Molecular Mass Distribution Measurement by Mass Spectrometry; Special Publication 960-21*, National Institute of Standards and Technology, Gaithersburg, Maryland, www.nist.gov/public_affairs/factsheet/practiceguides.cfm (last accessed: 8/11/2011).

105 Wallace, W.E., Flynn, K.M., Guttman, C.M., VanderHart, D.L., Prabhu, V.M., De Silva, A., Felix, N.M., and Ober, C.K. (2009) *Rapid Commun. Mass Spectrom.*, **23**, 1957–1962.

106 Park, E.S., Wallace, W.E., Guttman, C.M., Flynn, K.M., Richardson, M.C., and Holmes, G.A. (2009) *J. Am. Soc. Mass Spectrom.*, **20**, 1638–1644.

107 Kostanski, L.K., Keller, D.M., and Hamielec, A.E. (2004) *J. Biochem. Biophys. Methods*, **58** (2), 159–186.

108 Grubisic, Z., Rempp, P., and Benoit, H. (1967) *J. Polym. Sci. B Polym. Lett.*, **5**, 753–759.

109 Zammit, M.D. and Davis, T.P. (1997) *Polymer*, **38**, 4455–4468.

110 Zammit, M.D., Coote, M.L., Davis, T.P., and Willetto, G.D. (1998) *Macromolecules*, **31**, 955–963.

111 Tamai, Y., Konishi, T., Einaga, Y., Fujii, M., and Yamakawa, H. (1990) *Macromolecules*, **23** (18), 4067–4075.

112 Flory, P.J. and Fox Jr, T.G. (1951) *J. Am. Chem. Soc.*, **73**, 1904–1908.

113 Buback, M., Busch, M., and Lämmel, R.A. (1996) *Macromol. Theory Simul.*, **5** (5), 845–861.

114 Schnoll-Bitai, I. and Mader, C. (2006) *J. Chrom. A*, **1137** (2), 198–206.

115 Aaserud, D.J., Prokai, L., and Simonsick, W.J. (1999) *Anal. Chem.*, **71** (21), 4793–4799.

116 Prokai, L. and Simonsick, W.J. (1993) *Rapid Comm. Mass Spec.*, **7**, 853–856.

117 Tung, L.H. and Runyon, J.R. (1969) *J. Appl. Polym. Sci.*, **13** (11), 2397–2409.

118 Meira, G.R. and Vega, J.R. (2001) *Dekker Encyclopedia of Chromatography* (ed. J. Cazes), Marcel-Dekker, New York, p. 71.

119 Baumgarten, J.L., Busnel, J.P., and Meira, G.R. (2002) *J. Liq. Chromatogr. Rel. Technol.*, **25** (13–15), 1967–2001.

120 Mendel, J.M. (1995) Least-squares estimation: Singular-value decomposition, in *Lessons in Estimation Theory for Signal Processing, Communications and Control*, Prentice-Hall, New Jersey, pp. 44–57.

121 Reiter, J. (1992) *J. Comput. Phys.*, **103** (1), 169–183.

122 Skilling, J. and Bryan, R.K. (1984) *Mon. Not. R. Astr. Soc.*, **211** (1), 111–124.

123 Splinter, S.J. and McIntyre, N.S. (1998) *Surf. Interface. Anal.*, **26** (3), 195–203.

124 Shannon, C.E. (1948) *Bell System Tech. J.*, **27**, 379 & 623.

125 Shore, J.E. and Johnson, R.W. (1980) *IEEE Trans.*, **IT-26**, 26.

126 Shore, J.E. and Johnson, R.W. (1983) *IEEE Trans.*, **IT-29**, 942.

127 Sivia, D.S. (1996) *Data Analysis: A Bayesian Tutorial*, Oxford University Press, New York.

128 Itakura, M., Sato, K., Lusenkova, M.A., Matsuyama, S., Shimada, K., Saito, T., and Kinugasa, S. (2004) *J. Appl. Polym. Sci.*, **94**, 1101–1106.

129 Gridnev, A.A., Ittel, S.D., and Fryd, M. (1995) *J. Polym. Sci. A Polym. Chem.*, **33**, 1185–1188.

130 Wagner, H.L. and Hoeve, C.A.J. (1971) *J. Polym. Sci. A-2*, **9**, 1763–1776.

131 Koo, S.P.S., Junkers, T., and Barner-Kowollik, C. (2008) *Macromolecules*, **42** (1), 62–69.

132 Günzler, F., Wong, E.H.H., Koo, S.P.S., Junkers, T., and Barner-Kowollik, C. (2009) *Macromolecules*, **42** (5), 1488–1493.

133 Buback, M., Günzler, F., Russell, G.T., and Vana, P. (2009) *Macromolecules*, **42** (3), 652–662.

134 Crecelius, A.C., Baumgaertel, A., and Schubert, U.S. (2009) *J. Mass Spectrom.*, **44** (9), 1277–1286.

135 Giordanengo, R., Viel, S., Allard-Breton, B., Thévand, A., and Charles, L. (2009) *Rapid Commun. Mass Spectrom.*, **23** (11), 1557–1562.

136 Giordanengo, R., Viel, S., Allard-Breton, B., Thévand, A., and Charles, L. (2009) *J. Am. Soc. Mass Spec.*, **20** (1), 25–33.

137 Trimpin, S. and Clemmer, D.E. (2008) *Anal. Chem.*, **80** (23), 9073–9083.

138 Trimpin, S., Plasencia, M., Isailovic, D., and Clemmer, D.E. (2007) *Anal. Chem.*, **79**, 7965–7974.

139 Julka, S., Cortes, H., Harfmann, R., Bell, B., Schweizer-Theobaldt, A., Pursch, M., Mondello, L., Maynard, S., and West, D. (2009) *Anal. Chem.*, **81** (11), 4271–4279.

140 Nielen, M.W.F. and Buijtenhuijs, F.A. (1999) *Anal. Chem.*, **71** (9), 1809–1814.

141 Baumgaertel, A., Becer, C.R., Gottschaldt, M., and Schubert, U.S. (2008) *Macromol. Rapid Commun.*, **29** (15), 1309–1315.

Edited by C. Barner-Kowollik,
T. Gründling, J. Falkenhagen, S. Weidner

WILEY-VCH

Mass Spectrometry in Polymer Chemistry

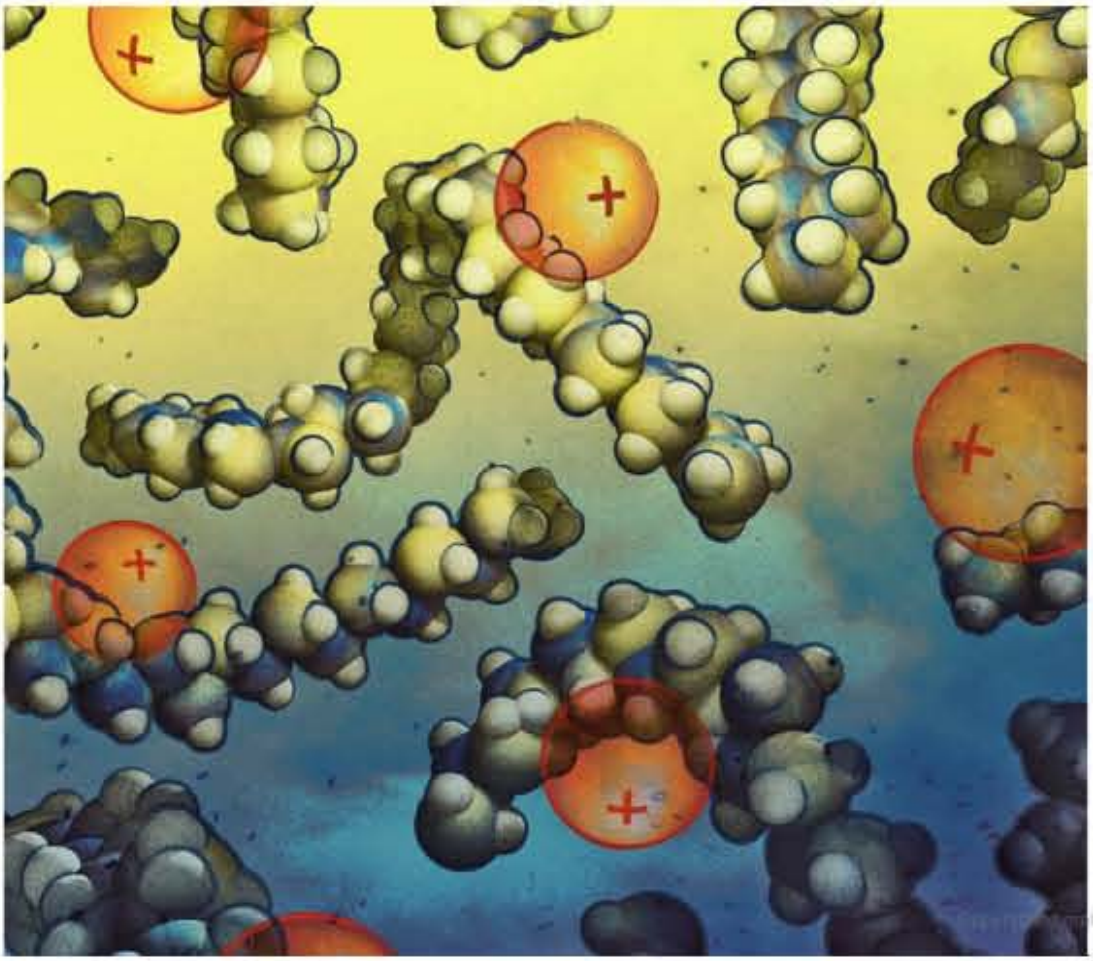

Edited by
Christopher Barner-Kowollik, Till Gruendling,
Jana Falkenhagen, and Steffen Weidner

Mass Spectrometry in Polymer Chemistry

WILEY-VCH Verlag GmbH & Co. KGaA

The Editors

Prof. Dr. C. Barner-Kowollik
Karlsruhe Institute of
Technology (KIT)
Engesserstr. 18
76128 Karlsruhe
Germany

Dr. Till Gruendling
Karlsruhe Institute of Technology (KIT)
Engesserstr. 18
76128 Karlsruhe
Germany

Dr. Jana Falkenhagen
Federal Institute for
Mat. Research & Testing (BAM)
Richard-Willstätter-Str. 11
12489 Berlin
Germany

Dr. Steffen Weidner
Federal Institute for
Mat. Research & Testing (BAM)
Richard-Willstätter-Str. 11
12489 Berlin
Germany

Cover:
Wiley-VCH thanks Gene Hart-Smith for the permission to use the cover illustration.

Library of Congress Card No.: applied for

British Library Cataloguing-in-Publication Data
A catalogue record for this book is available from the British Library.

Bibliographic information published by the Deutsche Nationalbibliothek
The Deutsche Nationalbibliothek lists this publication in the Deutsche Nationalbibliografie; detailed bibliographic data are available on the Internet at http://dnb.d-nb.de.

Cover Design Formgeber, Eppelheim

Typesetting Thomson Digital, Noida, India
Printing Fabulous Printers Pte Ltd, Singapore
Binding Fabulous Printers Pte Ltd, Singapore

Printed in Singapore
Printed on acid-free paper

Print ISBN: 978-3-527-32924-3
ePDF ISBN: 978-3-527-64184-0
oBook ISBN: 978-3-527-64182-6
ePub ISBN: 978-3-527-64183-3
Mobi ISBN: 978-3-527-64185-7